

BPM Systems Training (Ops) Hardware & Software

Arne Freyberger
Marie Keesee
Dianne Napier


February 14, 2005

Introduction

Dianne Napier




Why is the BPM System so important?

- Where's the beam?
 - BPMs are used to measure position of the electron beam in the beampipe for multipass and single pass operations.
 - BPM system includes 595 BPMs controlled by 2 different types of electronics, 4CH and SEE, distributed across a network of 32 IOCs.
 - Numerous systems and HLAPPS have been developed and depend on the BPM system.
- 



BPM Dependent Systems List


- Slow Orbit Locks
 - Energy Locks
 - Asymmetry Lock
 - Extraction Lock
 - Current Lock Program
 - Autosteer
 - Fast SEE
 - MOMod
 - FOPT
 - Yves/Chao Tools
 - FFB
 - Currant Snyder
 - 30Hz Hardware
 - 30Hz Sync
- A separate training class will be given for BPM Dependent Systems.
- 



BPM Systems Team


bpmteam@jlab.org

● Dianne Napier	Hardware System Owner	(napier@jlab.org)	x6239
● Richard Dickson	Software System Owner	(dickson@jlab.org)	x5082
● Arne Freyberger	Diagnostics System Owner/Integrator	(freyberg@jlab.org)	x6268
● Omar Garza	I&C Group Leader	(garza@jlab.org)	x7257
● John Musson	I&C Project Coordinator	(musson@jlab.org)	x7441
● Marie Keesee	BPM Software Support	(keesee@jlab.org)	x7635
● Ed Strong	nA BPM System Expert	(estrong@jlab.org)	x7229
● Keith Cole	nA & 4CH BPM Systems Lead Tech	(colek@jlab.org)	x5920
● Pete Francis	SEE BPM System & Beam Sync Lead Tech	(francis@jlab.org)	x7528
● Tony Delacruz	4CH BPM Support Tech	(delacruz@jlab.org)	x7029
● Darrell Spraggins	Operator	(spraggin@jlab.org)	x6070
● Tim Southern	Operator	(southern@jlab.org)	x6091





Lesson Plan Outline

- BPM Can
 - 4CH BPM System (Hardware)
 - SEE BPM System (Hardware)
 - Nomenclature & Equations (Software)
 - Planned Upgrades
 - Q & A
- 

Beam Position Monitor (BPM)

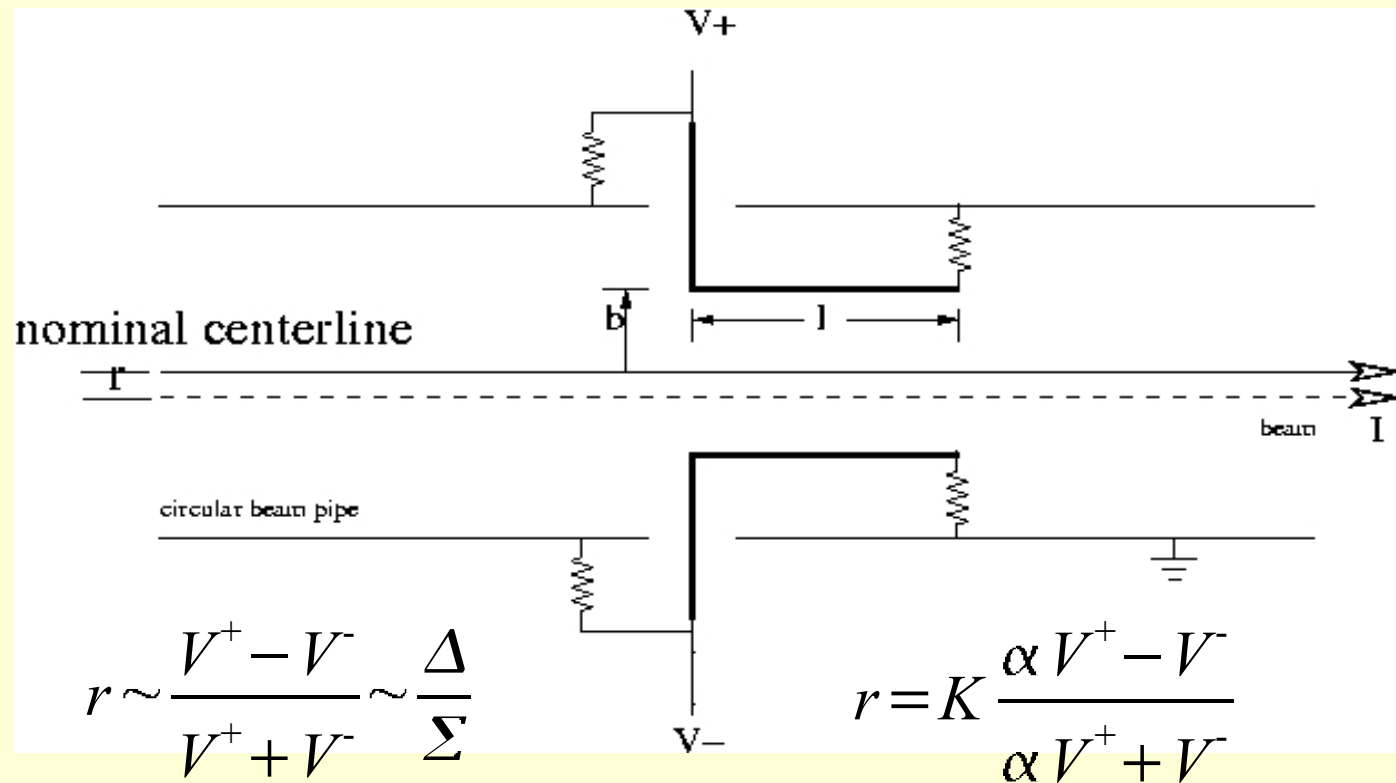
Arne Freyberger

Types

- **Antenna BPMs [the JLAB BPM]**
 - M15 [b=0.68"]
 - M20 [b=0.935"]
- **Stripline BPMs**
 - FEL cans used in some locations [spreader and recombiners]
- **Cavity BPMs**
 - nA BPMs in Hall-B
 - G0/Happex parity parameters



Antennae BPMs




$$l = \frac{3}{4} \lambda$$

- K is a sensitivity of the BPM, defined by its geometry:
 - M15: $K=18.81$, $b=0.68''$
 - M20: $K=25.67$, $b=0.935''$
- Alpha is the small difference in gains between the two electronics chains, this should be one for SEE electronics



Cavity BPM

- Electron beam produces a resonant standing field in a cavity.
 - Insert probes at the appropriate location to measure the power in the cavity
 - Position cavities measure the product of position and current
 - Lock-in amplifiers are used [analog nA system, digital G0/Happex] to obtain fantastic Signal/noise and dynamic range.
- 

Cavity BPM (cont.)

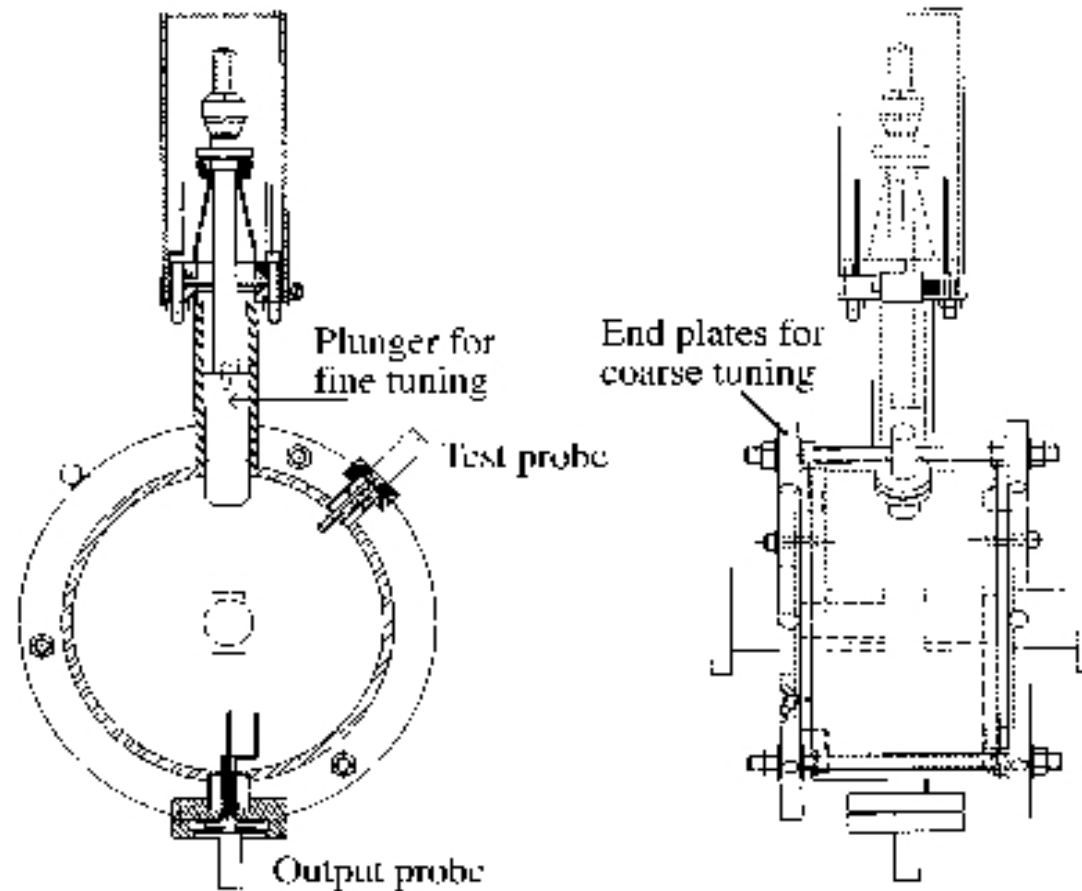
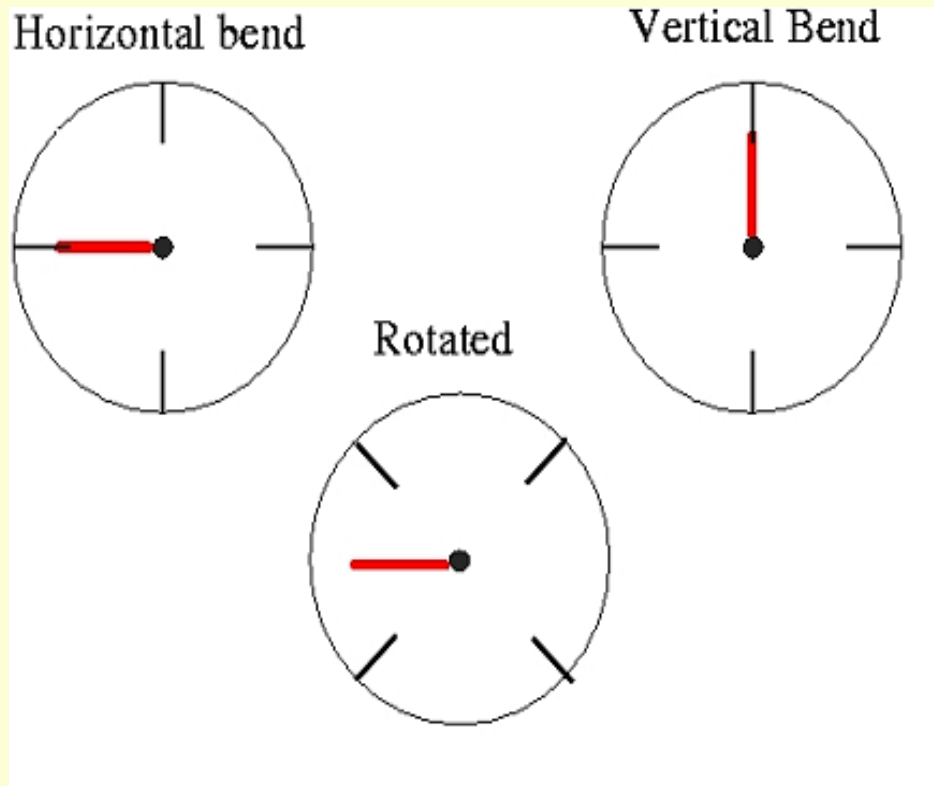


Figure 2. Position cavity front and side view.

Why are the BPM Cans Rotated?

- Antenna and Stripline BPMs are rotated to avoid the synchrotron light produced in the magnetic bends.



- With this rotation, in order to determine the X position, signals from all four pickups are used.

$$x = \frac{1}{\sqrt{2}} U + \frac{1}{\sqrt{2}} V$$

- where U and V are the measured rotated positions.




BPM Epics Name

- IPMgirder_name

- I: Instrument, P: Position, M: Monitor

- Except in the Linacs where one BPM measures up to five beam positions [in tune mode].

- The first digit in the girder name is replaced by the pass number (ie 0L01 becomes 0L01, 2L01, 4L01, 6L01, 8L01).
- 



BPM Epics Name (cont.)

● 1S00

- 1 = first pass east
 - 1, 3, 5, 7, 9 = east arc passes
 - 2, 4, 6, 8 = west arc passes
 - AL = 5th pass south linac
- S = spreader
 - I = injector
 - R = recombiner
 - T = transport
 - L = linac
 - A = arc
 - E = extraction
- 00 = girder location

● NL = North Linac
Long pulse
average

● SL = South Linac
Long pulse
average

● 1C = Hall A


● 2C = Hall B

● 3C = Hall C






History of the BPM System

- July 1990: 100MHz Tunnel Line Driver installed & tested in the injector.
 - This 100MHz system used in the Front End Test and commissioning of the North Linac.
 - Did not operate over a variety of beam currents
 - July 1990: 1497MHz Detector & Tunnel Amplifier tested in injector.
 - Requirements consisted of single pass detection, 1uA – 200uA beam current range, f_c of 1497MHz, and recirculation time of 4.2usec.
 - To be installed next to associated BPM with a gain stage to allow the signal to be transported several hundred feet to the service building without a serious degradation in the system noise figure.
 - ~1992: 1497MHz Detector or 4CH (4 Channel) BPM system was developed and installed in the east arc to commission the North Linac.
 - January 1993: Studies of the Linac BPMs (100MHz system) were conducted. RF feedthrough was being detected by the system and reported as a position – needed a new system.
 - In order to tune up the machine and perform periodic orbit corrections, it is necessary to track beam position through the entire five pass orbit. 4CH BPM system accomplished this system in the arcs, but could not detect multipass beam in the Linacs.
 - 1995: SEE (Switched Electrode Electronics,) designed by T. Powers, were installed in the Linacs
 - 2000: 4CH System cannot detect G0. Muxed SEE system was installed in the east and west arc.
- 



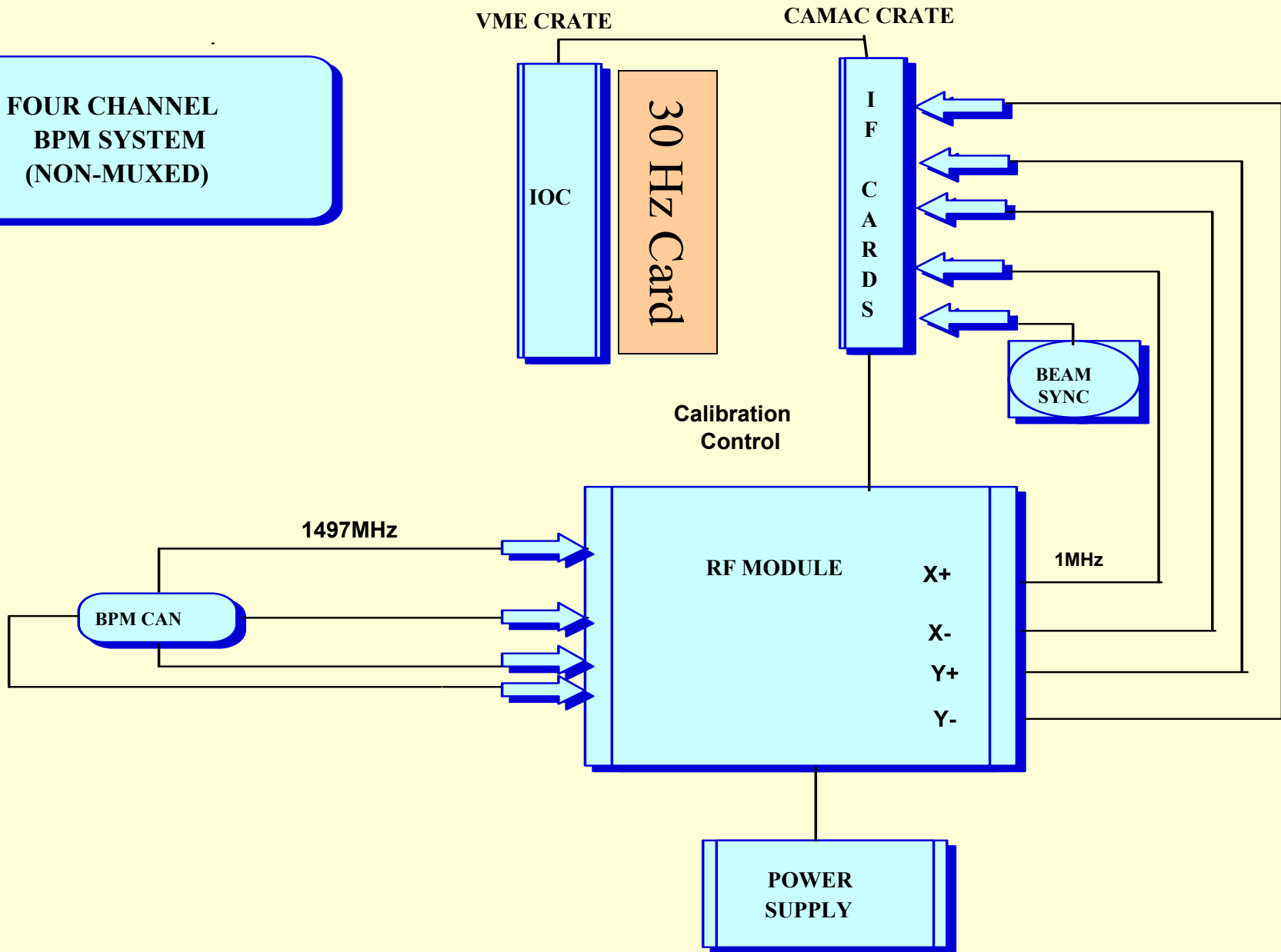
BPM Types

- **1nA** – the 1nA BPMs are the cavity type BPMs in Hall B that can read low currents down to the pA range.
 - nA BPM system will be covered in a separate training class.
 - **4CH** – BPMs located in the arcs that use the 4ch electronics. Their current range is 1uA to 200 uA.
 - **SEE – Switched Electrode Electronics**
 - **SLN** – SEE BPMs that use the Linac style of electronics. The SLN type of SEE BPM is intended for multipass linac locations and has a current range of 1uA to 1000uA.
 - **STP** – SEE BPMs that use the Transport style of electronics. The STP type of SEE BPM is intended for transport locations with a current range of 100nA to 200uA.
 - **SMX** – SEE BPMs that have the inputs to the front end electronics hardware multiplexed and use the Transport style of electronics. This type is found only in the arcs.
- 

4CH BPM System

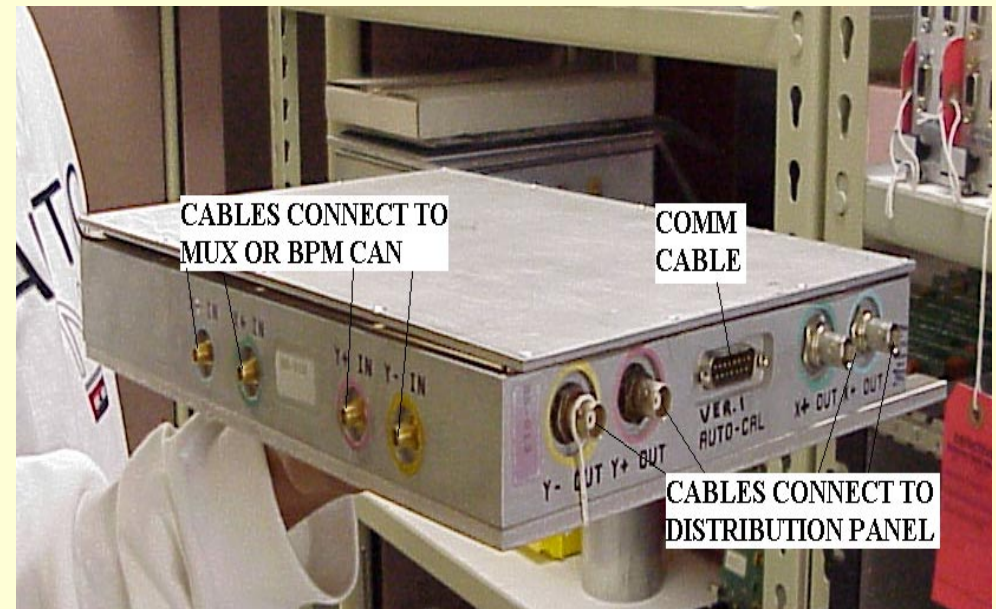
Dianne Napier

**FOUR CHANNEL
BPM SYSTEM
(NON-MUXED)**




RF Module Description

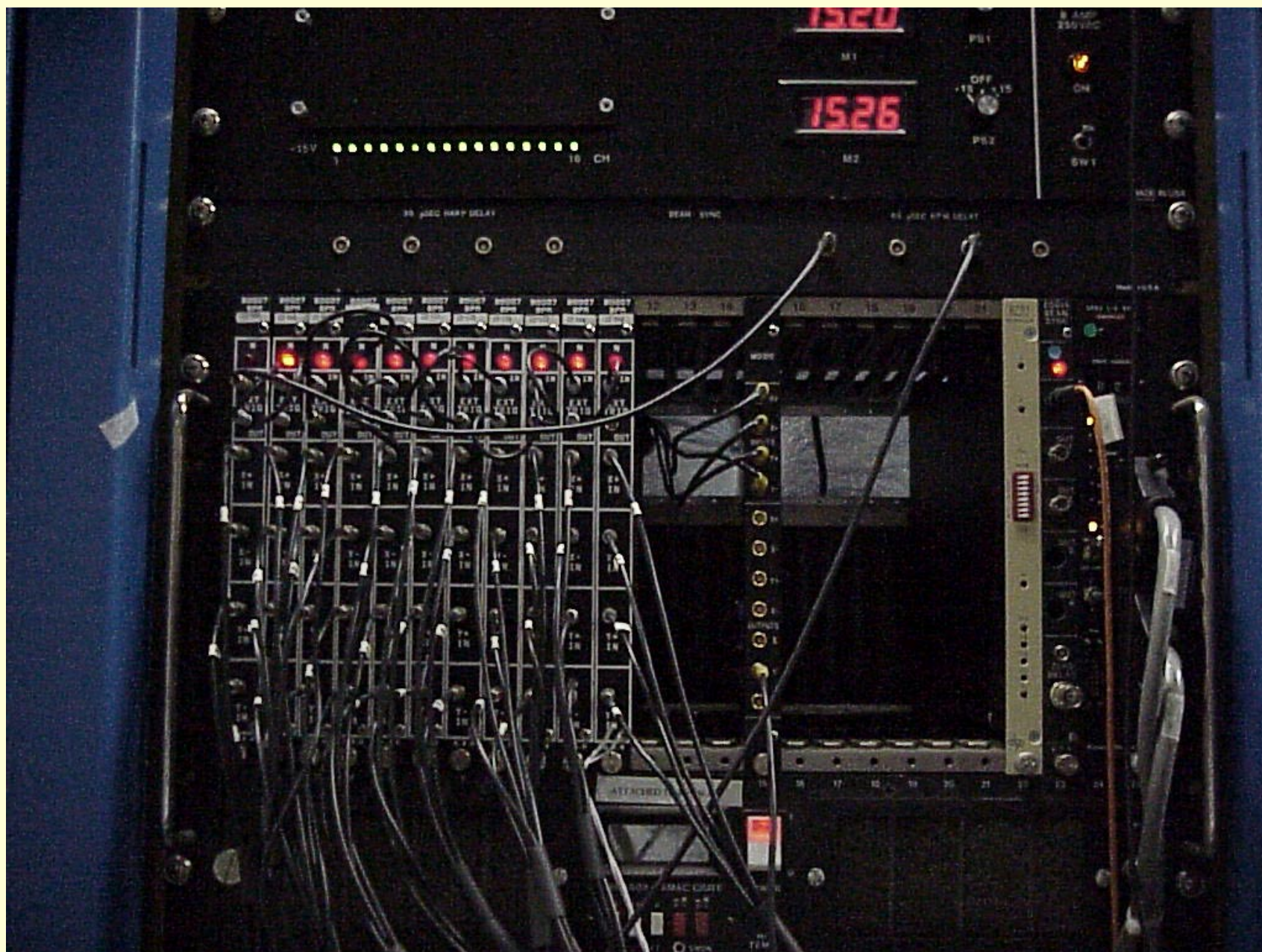
- AKA: Tunnel Electronics, Down Converter, B0005 Detector, B0148 Detector
- 4 channel (X+, X-, Y+, Y-) 1.497GHz RF front-end amplifier with a down-converted 1MHz IF, and IF amplifier
- Has a 2 channel internal RF calibration source (1.497GHz)
- Sends signals @1MHz to IF Card for processing
- Located in the tunnel



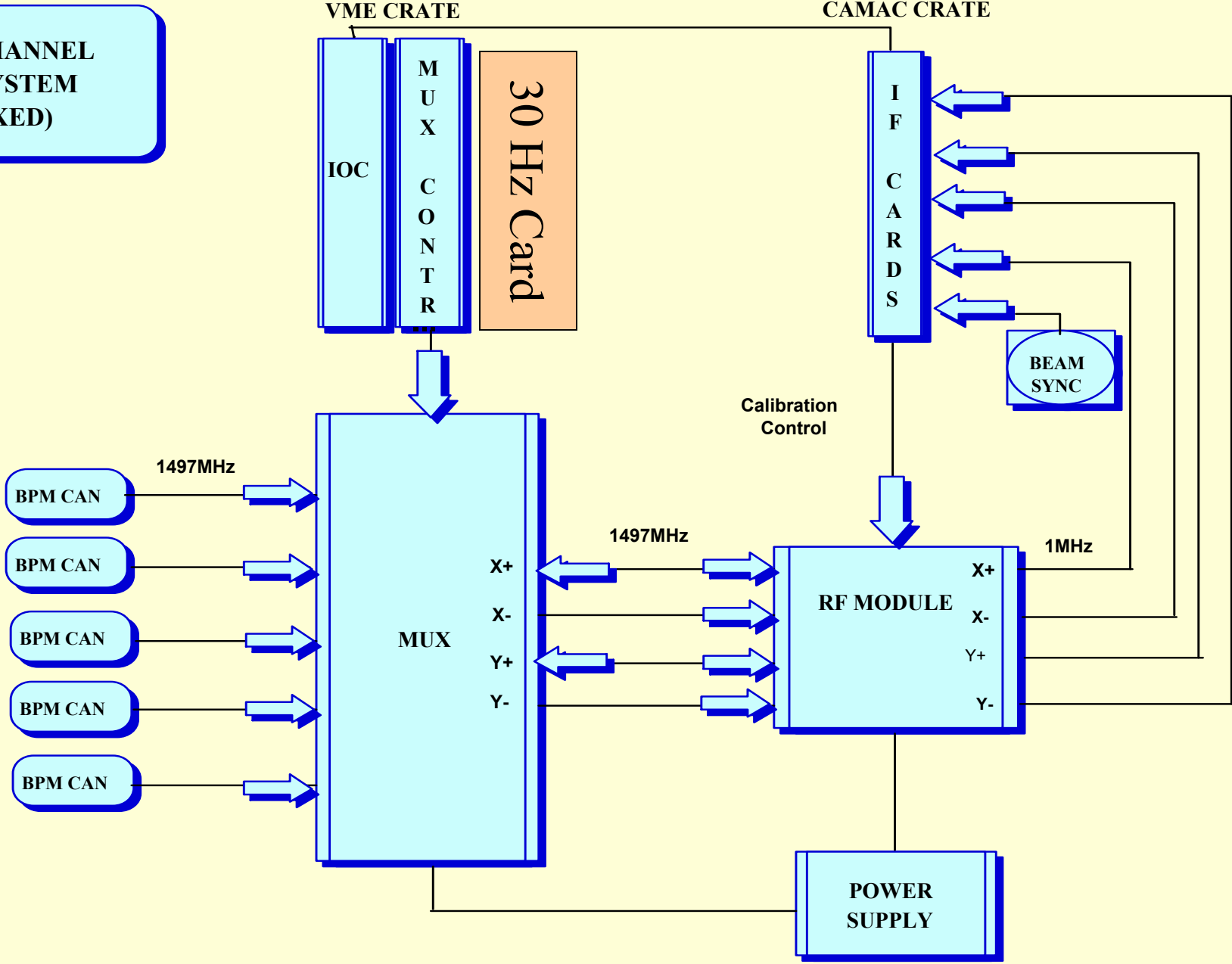


IF Card Description

- 1MHz Detector Board
 - CAMAC based; resides in the service buildings
 - Resolves the Four 1MHz signals from RF Module to a dc level & converts to a 12-bit word
 - Handles auto-calibration; sends commands to the RF Module to turn on calibration and settings to vary the strength of the calibration signal (cal signal level)
 - Has a variety of gain settings (GCV; Gain Control Voltage) for various input signals
 - Can run in pulse and continuous modes
 - Sends signals serially to the master controller, VME-based Motorola CPU and then to software
 - Beam Sync (60Hz) input used as a trigger for data acquisition
- 

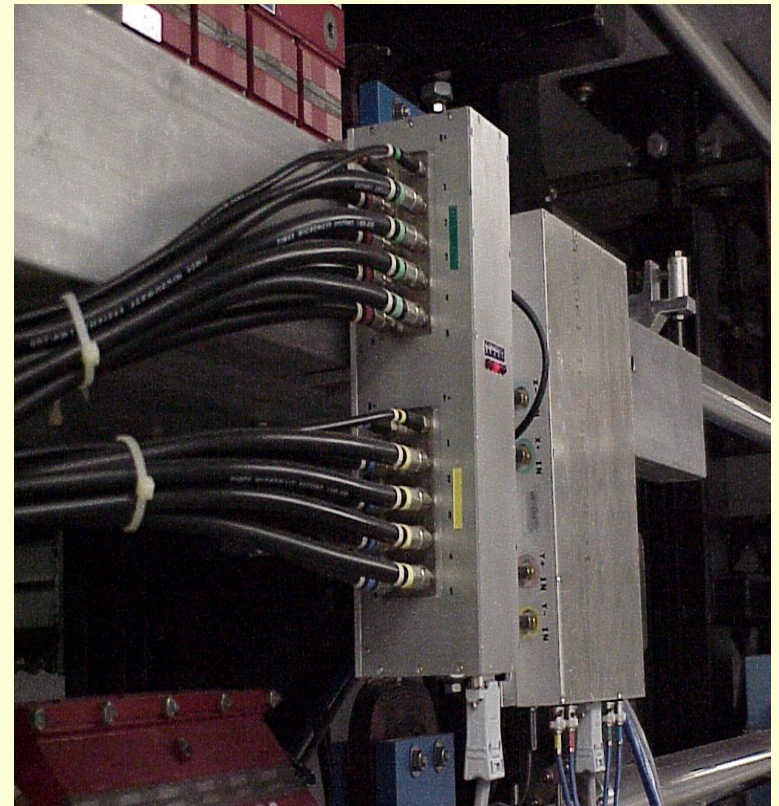


**FOUR CHANNEL
BPM SYSTEM
(MUXED)**



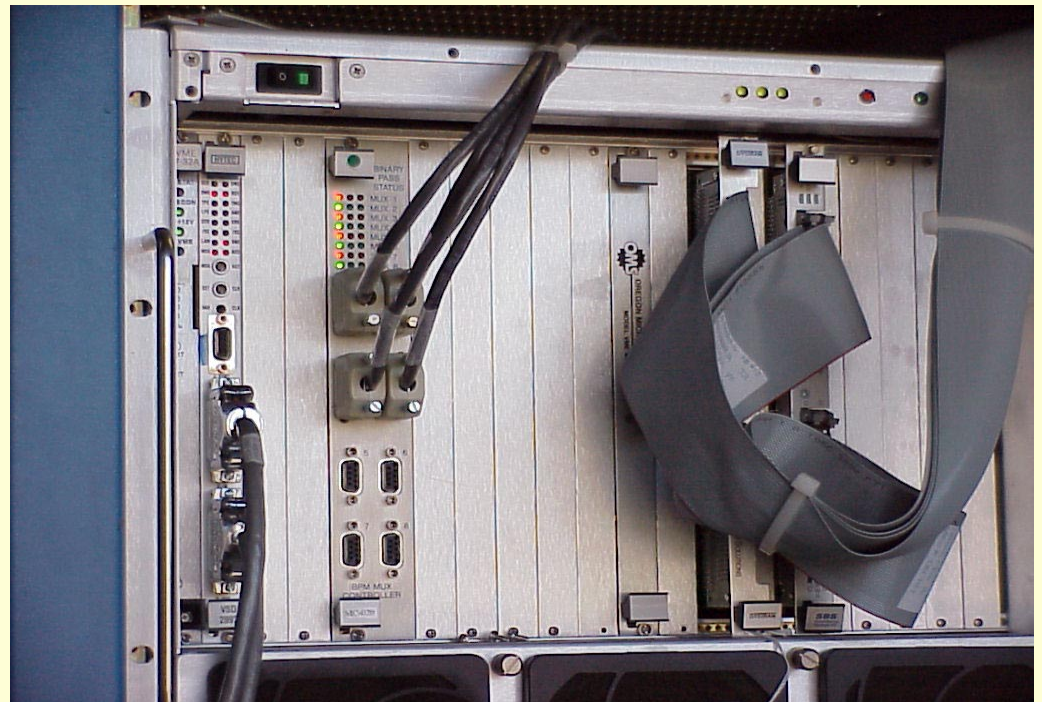
Mux Description

- Capable of multiplexing between 5 BPM cans
- Switches from pass 1 through 5
- Sends signals @ 1497MHz to RF Module
- 2 types: Old Style (as shown) & Supermux
 - Supermux is a redesign of the old style; has greater pass to pass isolation; more reliable




Mux Controller Description

- VME based; capable of controlling 8 muxes
- Controls Mux & defines which pass the mux will monitor






30Hz Card Description

- Part of the TSS (Timing Synchronization System) or Synch30Hz
 - Clock Module, VME based, can be master or slave
 - As master, sends out messages in response to an external synchronization signal over a serial fiber optic line
 - As a slave, receives the messages and interrupts an associated computer in its VME crate
 - The Synch30Hz application derives the timing information from a fiber optic data link from master card located in iocmc1.
 - During normal ops, the 4ch software acquires a signal from the Synch30Hz software coincident with the beam sync arrival. Since the 4ch BPM hardware is triggered by the beam sync, this allows the software to acquire the data from the hardware at the proper time.
- 



System Requirements: Specifications & Beam Type

- Single pass beam operations
 - Electron beams of different energy travel in 5 different paths in the east and west arc regions of the Accelerator.
 - BPMs measure the beam position for each of the 5 paths.
 - Range: $1\mu\text{A}$ – $200\mu\text{A}$ with +/- 0.5mm accuracy
 - Beam Type
 - Will respond to pulsed beam (tune beam)
 - Current Dependent
 - $1\mu\text{A}$ – $200\mu\text{A}$ with +/- 0.5mm accuracy
 - Will not respond to G0 Laser
 - G0 beam structure saturates the RF Module
 - Will not respond to Hall B Laser
 - Current too low.
 - For economical reasons, (up to 5) BPMs are muxed.
 - Must have Beam Sync & Synch30Hz
- 



System Requirements: Locations

- Locations
 - East and West Arcs
 - FEL




SEE BPM System

Dianne Napier



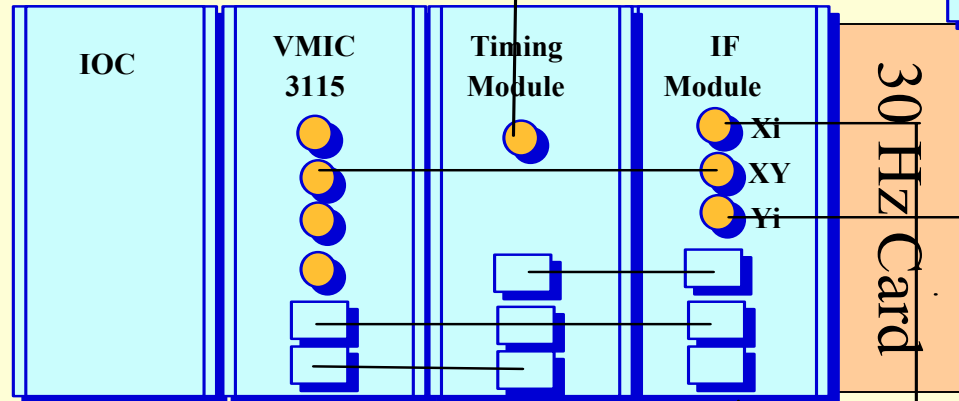
Why another BPM System?

- SEE (Switched Electrode Electronics) was developed b/c the 4CH BPM System could not detect multipass beam, has a limited range of 1uA – 200uA beam current, & suffers from differing drifts in the gain between the plus and minus channels for each beam axis.
 - Provides +/- 0.1mm accuracy with position range of +/- 5mm with higher dynamic range in beam current.
 - Has a pulsed multipass detection scheme which is achieved by tuning the SEE timing to match the machine recirculation period of 4.237us (beam pulse of 4.2us allows system to resolve the components of a multipass beam in the linacs).
 - Developed in 1994 by Tom Powers and installed in Spring 1995
- 

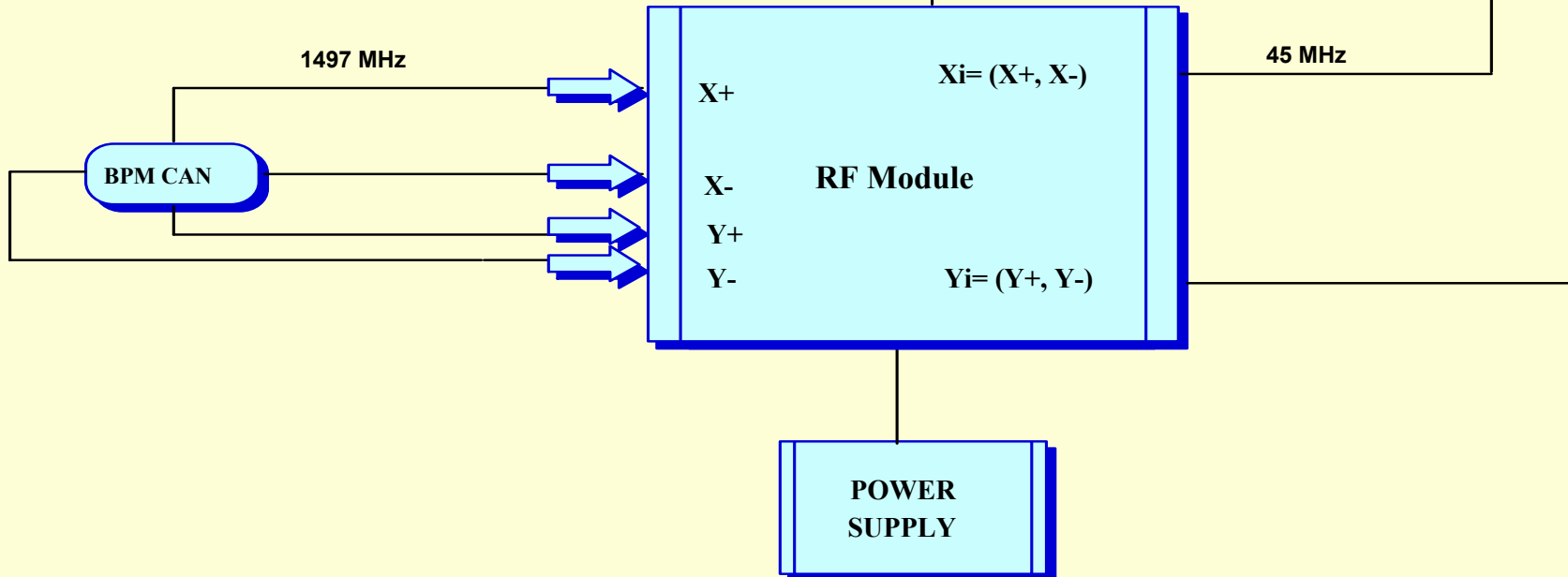
SEE BPM SYSTEM
(NON-MUXED)

VME CRATE

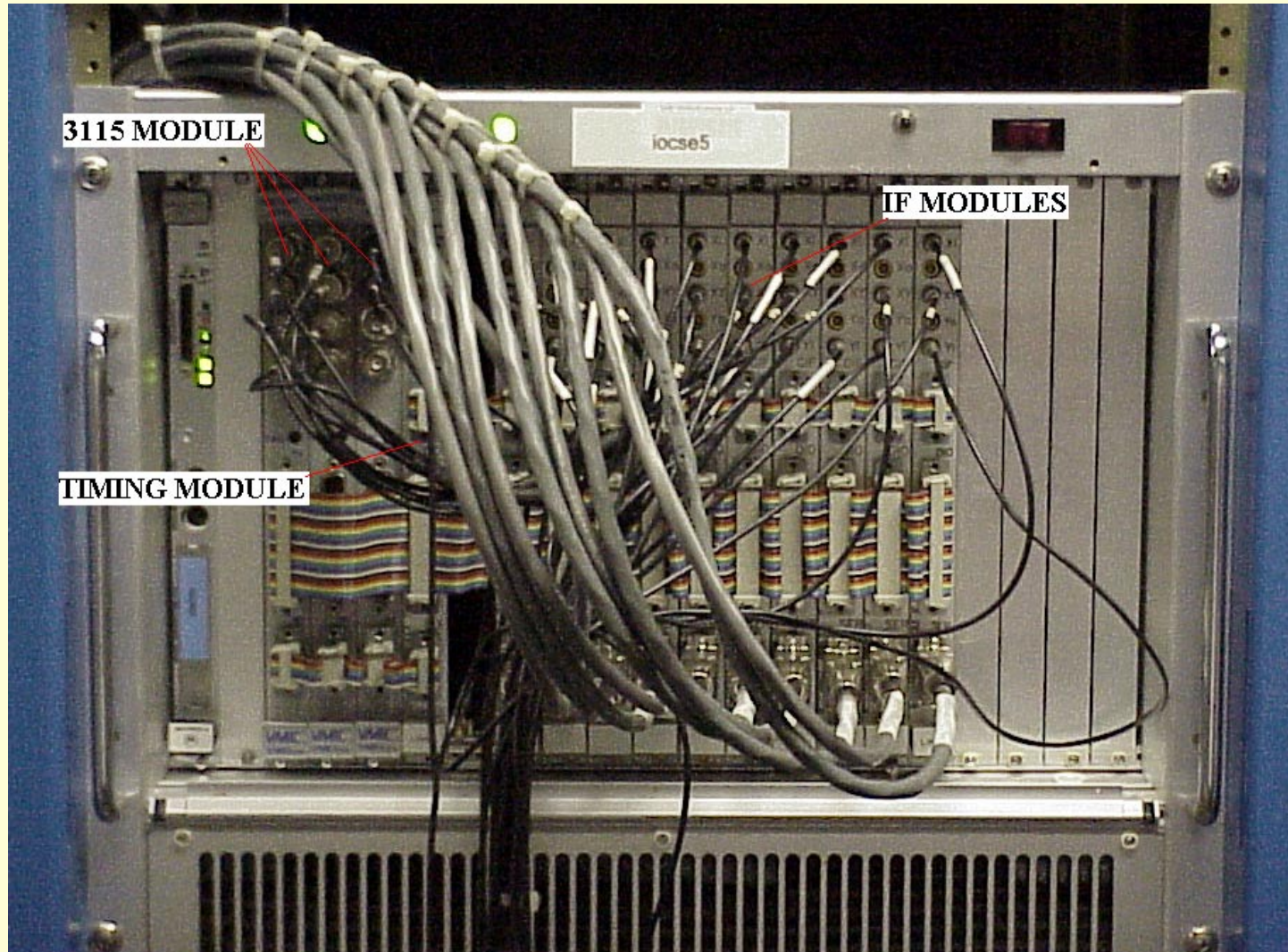
BEAM
SYNC



Comm/Gain Control/
Calibration Control

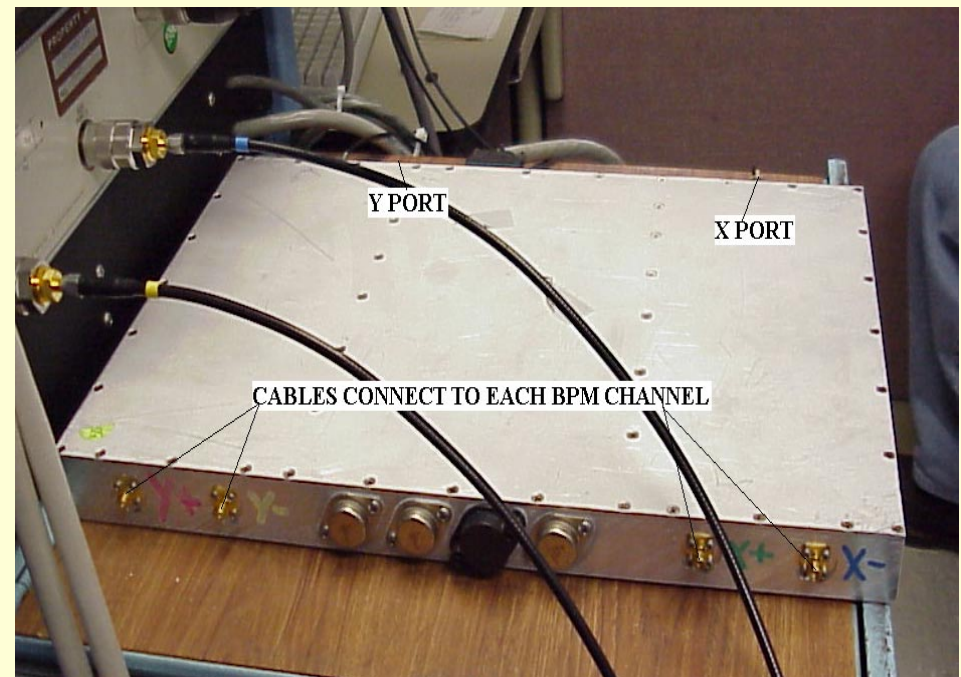


SEE Hardware Field Shot




RF Module Description

- Amplifies & down converts 1497MHz to 45MHz
- (X+,X-) & (Y+,Y-) are time-domain multiplexed into one signal (X) & (Y), respectively
- Sends signals @45MHz to IF Module
- Up to 12 per IOC
- Located in the tunnel






IF Module Description

- VME based
 - Up to 12 per IOC
 - Amplifies, filters, down converts to a base band signal, filters again, and multiplexes 45MHz signals as X+Y+X-Y- data
 - Uses a multiplexing technique (multiplexes the plus and minus signals on the BPM plane) to insure that the gain changes and offsets on the RF, and IF and base band chains do not affect the position calculation. This is to minimize the number of ADC channels (signals sent to the 3115 Module).
 - Input range of -59dBm to -27dBm
 - Has 4.2us cycle time
 - 3 analog outputs [2 (X0 and Y0) for sample and hold modules, 1 (XY) for the 3115 module].
- 




Timing Module Description

- VME based
 - 1 per IOC
 - Synchronizes BPM position data by generating specific timing signals to the IF Modules, RF Modules, and 3115 Module with help of externally provided Beam Sync signal
- 




3115 Module Description

- VME based
 - Up to 3 per IOC
 - ADC
 - Receives XY signal from IF card
 - Can accept up to 4 analog inputs from 4 separate IF cards
- 




30Hz Card Description

- Same card as used with 4CH BPM System
 - Part of the TSS (Timing Synchronization System) or Synch30Hz
 - Clock Module, VME based, can be master or slave
 - As master, sends out messages in response to an external synchronization signal over a serial fiber optic line
 - As a slave, receives the messages and interrupts an associated computer in its VME crate
 - The Synch30Hz application derives the timing information from a fiber optic data link from master card located in iocmc1.
 - The BPM software uses information from the Synch30Hz application to synchronize the data acquisition software with the BPM hardware.
- 



Sample and Hold Module Description

- VME based
 - For user community, can use their own data acquisition hardware to acquire and process the beam position
 - Not required for SEE System to function
 - De-multiplexes and filters the positive/negative signals from the IF Module
 - Inputs:
 - 2 signals (X0 and Y0) from 1 IF Module
 - Beam Sync signal; GIF (gated integrating filter signal) and Trigger signal from Timing Module
 - These 3 are used to generate the signals required to the sample and hold amplifiers that de-multiplex the X0 and Y0 signals from the IF Module into X+, X-, Y+, and Y-.
- 




SLN & STP

● SLN: SEE Linac Type

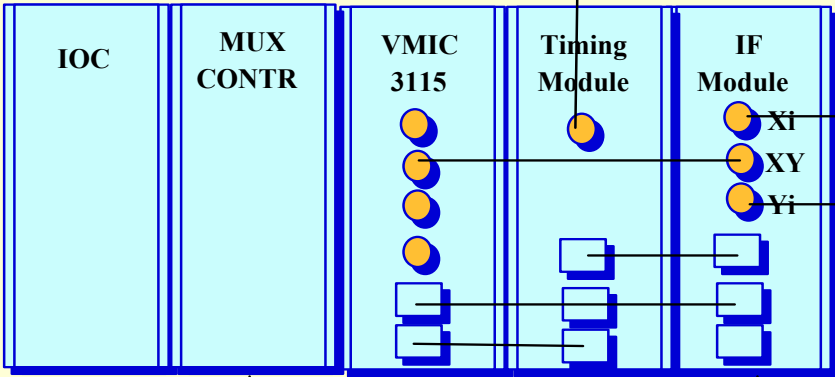
- 1uA – 1000uA beam current
- Used in Linac regions (multipass operation) & FEL (0.5uA – 2000uA)
- RF Module gain is 25dB
- IF Module has 4.237us switching time
- Timing Module has 8.496us (2x machine circulation) base timing cycle

● STP: SEE Transport Type

- 100nA – 200uA
 - Used in Transport regions (one pass operation) and arcs (SE7, SE13)
 - RF Module gain is 38dB
 - IF Module has 70us switching time
 - Timing Module has 140us base timing cycle
- 

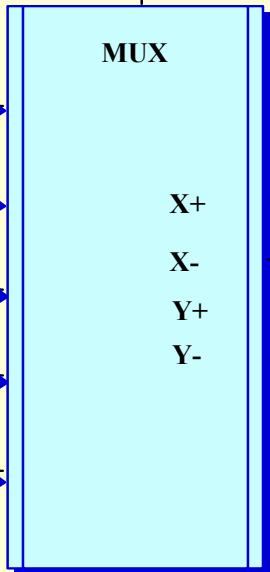
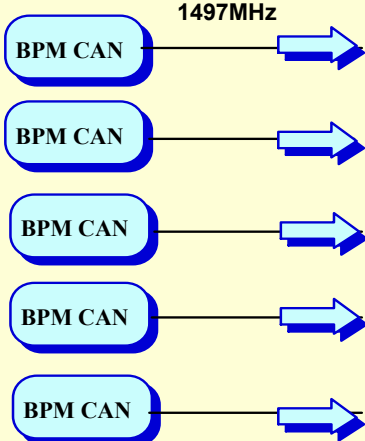
SEE BPM SYSTEM
(MUXED)

VME CRATE

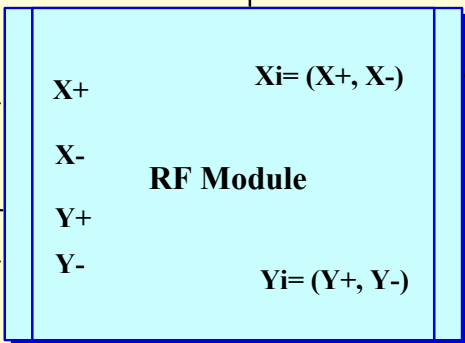


BEAM SYNC

30 Hz Card



4CH POWER SUPPLY



SEE POWER SUPPLY

Comm/Gain Control/
Calibration Control

45 MHz

1497MHz



Mux & Mux Controller Description

- Same as 4CH BPM System






SMX (STP Muxed)

- SMX (SEE Muxed System)
- Consists of STP (SEE Transport Type) electronics






System Requirements: Specifications & Beam Type

- +/- 0.1mm accuracy with position range of +/- 5mm with higher dynamic range in beam current
 - Current Dependent
 - Detects beam intensity levels in 3 different ranges
 - Range 1: Linac Style (1 μ A-1000 μ A)
 - Range 2: Transport Style (100nA-200 μ A)
 - Range 3: Hall B Transport Style (200pA)
 - 1nA BPM system is used
 - All beam types including G0
 - Has been tested to report 50nA (Hall B Beam)
 - Requires snake pulse for multipass detection
 - Some lasers do not have this snake pulse in tune mode
 - Must have Beam Sync and 30Hz Sync
- 



System Requirements: Locations

- SLN (SEE Linac Style): Linacs & part of Hall A
 - STP (SEE Transport Type): Injector, BSY, Halls
 - SMX (SEE Transport Type – Multiplexed): East and West Arc (IOCSE7, IOCSE13)
- 

Nomenclature & Equations

Marie Keese




BPM Position Equation

Note: The following equations are for the X (Horizontal) component of the BPM positions. The Y (Vertical) component equations are done the same way with the Y wire signals, calibration constants, and offsets.

$$XROT = k \frac{(X_p - X_{offp}) - \alpha_x (X_m - X_{offm})}{(X_p - X_{offp}) + \alpha_x (X_m - X_{offm})}$$

$$XRAW = XROT * \cos(45^\circ) + YROT * \sin(45^\circ)$$

$$YRAW = YROT * \cos(45^\circ) - XROT * \sin(45^\circ)$$


- The position, **XRAW**, is obtained by rotating 45 degrees (some exceptions in Injector and FEL)
 - **K** is the sensitivity of the BPM can
 - **X_p** is the signal from the positive X wire and **X₋** is the signal from the negative X wire
 - **X_{offp}** is the positive wire offset, determined during calibration with beam and cal signal off
 - **X_{offm}** is the negative wire offset, determined during calibration with beam and cal signal off
 - **α_x** is the relative gain ratio determined during calibration
- 



BPM Positions and Offsets

$$XPOS = XRAW - (XSOFF + XGOF)$$

XPOS and YPOS are the positions displayed on the absolute spike screens.

- **XRAW** – the resulting position (in mm) after rotating the XROT position 45 degrees.
 - **xsof** - survey offsets – used to calibrate the BPMs electrical center relative to an adjacent physical device. There are 2 cases: magnetic center of quadrupoles and edge of YA septa magnets.
 - **xgof** - general offset – shift the horizontal position in the arcs to add or subtract path length.
- 



BPM Positions and Offsets (cont.)


$$XPRL = XPOS - XPOF$$

XPRL and YPRL (Relative Positions) are the positions displayed on the relative spike screens.

- **xpof** – relative position offset - is set to the X position when a Zero Pos is performed.

$$XGRL = XPOS - XGLD$$

XGRL and YGRL (Gold Positions) are the positions displayed on the Gold relative spike screens.

- **xgld** - gold offset – is used to obtain the gold positions that indicate the ideal trajectory for the beam. This is not fully developed yet.
- 



BPM Positions and Offsets (cont.)

$$XDRP = XDAP - XDPO$$


XDRP and YDRP (relative 30 Hz positions) are displayed on the Relative 30 Hz spike screens.

- **xdpo** – 30 Hz relative position offset - is set to the 30 Hz X position when a 30 Hz Zero Pos is performed.





BPM Calibration


- The SEE and 4ch BPM systems have calibration routines. The 4ch calibration routine is called Supercal. The SEE calibration routine is referred to as alpha calibration.
 - The two tasks of the calibration routines are:
 - To determine the wire offsets with the calibration signal and the beam off.
 - To determine the alpha value for the X and Y channels.
 - The constant, alpha, is the relative gain ratio of the + and – wires for each channel.
 - The only signal source during the alpha calibration should be from the calibration signal (i.e. beam should be off).
- 



Alpha Calibration Equation

$$\alpha_x = \frac{X_p - X_{offp}}{X_m - X_{offm}}$$


Where

- X_p and X_m are the wire signals with beam off and the calibration signal on
 - X_{offp} and X_{offm} is the offset determined with the beam and calibration signals off
- 



BPM Timing


Data Acquisition Timing

- The BPM software uses information from the Synch30Hz application to synchronize the data acquisition software with the BPM hardware.
 - The Synch30Hz application derives the timing information from a fiber optic data link from iocmc1.
 - During normal ops, the 4ch software acquires a signal from the Synch30Hz software coincident with the beam sync arrival. Since the 4ch BPM hardware is triggered by the beam sync, this allows the software to acquire the data from the hardware at the proper time.
 - During normal ops, the SEE software gets an interrupt from the SEE hardware to tell it when to get the data.
 - Both systems acquire the necessary polarity information from the Synch30Hz application to correctly acquire and process the data when the 30 Hz system is operating.
- 

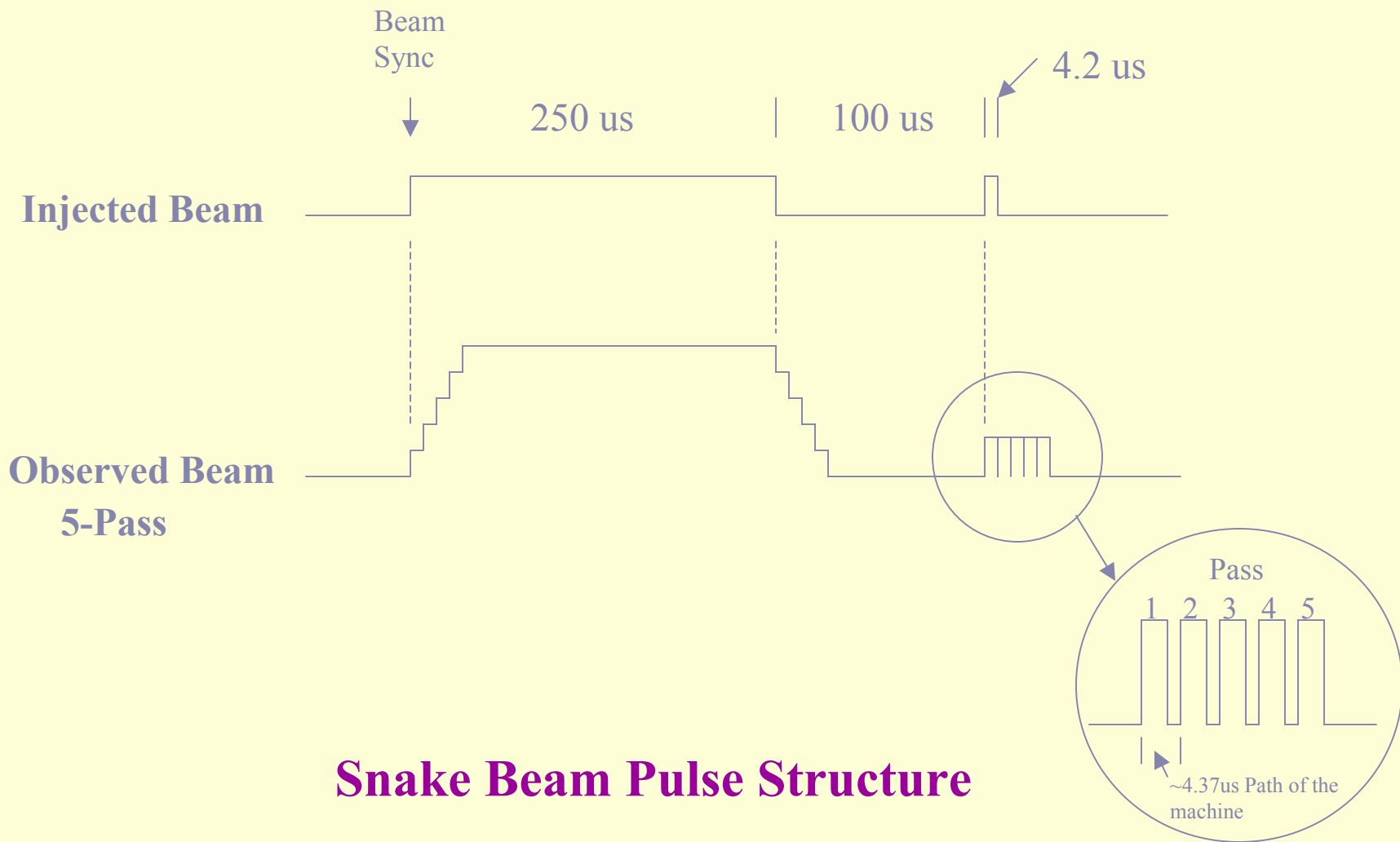


BPM Timing (cont.)

Linac Multi-pass Positions (SEE only)

- In the linacs, there is one beam pipe (and hence one BPM can) with up to 5 beams going through it.
 - The BPM software, in tune (pulsed) mode, makes use of the snake pulse structure to distinguish between the individual beams.
 - Since the software knows where, in time, the 4.2 us pulse for each pass is located in the data acquisition buffer, it is able to calculate each pass's position based only on that pass's data.
 - The “Long Pulse Average” position is calculated with the data from the first 250us pulse.
- 


BPM Timing (cont.)



Snake Beam Pulse Structure



30 Hz Positions

- When the accelerator 30Hz system is operating, 30Hz positions can be viewed on the 30Hz spike screens.
 - The 30 Hz positions are calculated by subtracting the positive modulation positions from the negative modulation positions during each data acquisition cycle.
 - The Synch30Hz application generates the 30 Hz modulation signal and passes the polarity information to all of the BPM IOCs in the machine.
- 

Planned Upgrades

Marie Keese




Planned Upgrades

Upgrades for this downtime:

- Add a BPM alarm handler with guidance for the various alarms.

Future Upgrades:

- Add an alarm for “Bad Tune Structure”. This alarm will indicate when the tune mode “snake” pulse structure is incorrect.
 - Upgrade the BPM History Editor to look and act more like the RF History Editor.
 - Add low current mode for the SEEs that will detect Hall B beam.
 - Global SEE calibration tool.
- 




References

● **Technotes (document titles below are clickable links)**

- Powers, T. et al., “Design, Commissioning and Operational Results of Wide Dynamic Range BPM Switched Electrode Electronics”, Proceedings of the Seventh Beam Instrumentation Workshop.
- Powers, T., “Improvement of the Noise Figure of the CEBAF Switched Electrode Electronics BPM System”, TN#98-05
- Hofler A. et al., “Performance of the CEBAF Arc Beam Position Monitors”, Proceedings of the Particle Accelerator Conference, Washington DC. 1993.
- Hofler, A., “How the Linac Beam Position Monitors Work”, TN#93-004
- Barry, W., “A General Analysis of Thin Wire Pickups for High Frequency Beam Position Monitors”.
- Keesee, M. et al., “The Timing Synchronization System at Jefferson Lab”, PSN# TUAP070.

● **Other documents:**

- Powers, T., “Differences between linac style and transport line style SEE systems”, 1997.
 - Powers, T., “SEE Sample and Hold Module Description”.
 - Powers, T., “SEE Software Requirements Documentation Rev. b”.
 - Denard, J-C., “IF Board B0007 Test Procedure Rev 1B”, April 1999.
- 

Q & A



Design, Commissioning and Operational Results of Wide Dynamic Range BPM Switched Electrode Electronics*

Tom Powers, Lawrence Doolittle, Rok Ursic and Jeffrey Wagner

*Continuous Electron Beam Accelerator Facility,
12000 Jefferson Ave., Newport News, VA 23606*

Abstract. The Continuous Electron Beam Accelerator Facility (CEBAF) is a high-intensity, continuous wave electron accelerator for nuclear physics. Total acceleration of 4 GeV is achieved by recirculating the beam through two 400 MeV linacs. The operating currents, over which the linac beam position monitoring system must meet specifications are 1 μ A to 1000 μ A. A system was developed in 1994 and installed in the spring of 1995 that switches four electrode signals at 120 kHz through two signal conditioning chains that use computer controlled variable gain amplifiers with a dynamic range greater than 80 dB. The system timing was tuned to the machine recirculation period of 4.2 μ s so that components of the multipass beam could be resolved in the linacs. Other features of this VME based system include long term stability and high speed data acquisition, which make it suitable for use as both a time domain diagnostic tool and as part of a variety of beam feedback systems. The computer interface has enough control over the hardware to make a thorough self-calibration and verification-of-operation routine possible.

INTRODUCTION

The CEBAF accelerator linacs are designed to operate with linac currents ranging from 1 μ A to 1 mA. The beam position monitoring (BPM) system is required to detect the beam with a relative accuracy of 100 μ m for a position range of ± 5 mm. It must maintain this accuracy during both pulsed and CW operation. It was also required that the system have the capability of distinguishing the position of each of the five beamlets during pulsed operation for machine tune-up. Additionally, a technique to determine the position of the 5 beamlets during CW operation was desired.

The original BPM electronics [1] which were used for commissioning the machine did not have sufficient dynamic range to operate at total currents outside of a range between 10 μ A and 100 μ A. This four channel system suffers from differing drifts in the gain between the plus and minus channels for each beam axis. Additionally, there are no provisions for detecting multipass beam. The switched electrode electronics beam position monitoring (SEE BPM) system described in this paper overcame problems encountered with the previous BPM system by employing a single amplifier-detector chain for each of the two X and Y channels. Many of the features of the system described in this paper have been used in similar systems developed at other laboratories.[2, 3, 4, 5] The significant feature of this systems is its pulsed multipass detection scheme which is achieved by tuning the SEE timing to match the machine recirculation period of 4.237 μ s. This along with operating the machine with 4.2 μ s pulsed beam allowed us to

resolve the components of a multipass beam. This same type of operation can be used to detect the difference in the beam centroid when an inverse snake (a reduction in beam current for 4.2 μ s) is applied to the CW beam.

*Supported by DOE Contract #DE-AC05-84ER40150

SYSTEM REQUIREMENTS AND PERFORMANCE

The design team started with the requirements summarized in table 1. The dynamic range is defined as the range of currents for which the system operates within all other specified limits. At the end of the design phase the performance of the hardware was measured on the bench and to a lesser extent in the machine. The high current end of the dynamic range will be tested on the machine when it is operated at rated currents. Laboratory testing indicates that the lower end of the dynamic range is limited by thermal noise. The high end is limited by signal compression in the electronics. The current dependence, beam position range and rms fluctuation measurements are also based on laboratory measurements which have not been refuted by operating experience.

Table I. Requirement and performance specifications

	Requirement specification	Performance specification
Dynamic range	1 - 1000 μ A	0.4 - 2000 μ A
Nominal measuring rate out of control system	1 meas./s	1 meas./s
Beam position range	$ x , y \leq 5$ mm	$ x , y \leq 5$ mm
Resolution (rms. fluct. at nominal meas. rate)	≤ 0.1 mm	≤ 0.1 mm
Current dependence	≤ 0.1 mm	≤ 0.1 mm
Multipass capability	some kind	"snake" pulse
Measuring bandwidth	10 – 100 kHz	120 kS/s

SYSTEM DESCRIPTION

The installed linac SEE BPM system consists of six VME crates each controlling seven to ten BPM channels (56 channels total). These crates are located in the service buildings approximately 10 meters above the beam line. Each channel consists of a BPM detector, an RF module located in the tunnel and an IF module located in the VME crate. Each crate has a timing module which is used to synchronize the system to the accelerator and generated specific timing signals required by the IF, RF and data acquisition modules. The VME crate also contains three commercial data acquisition modules and a single board microcomputer which are used to acquire and process the position signals prior to transmitting them to the machine control system.

RF Module

The detector in the system is a four wire stripline antenna system previously described [6]. It is connected to a four-input (X+, Y+, X-, and Y-) two-output (X

and Y) RF module, which is located about 1 m off of the beam line axis. The RF module switches between the plus and minus channels; amplifies the signal by 23 dB if necessary; down converts the 1497 MHz RF signals to 45 MHz; and transmits them to the IF module via coaxial cables. The range of input signals for the RF module is -77 dBm to -11 dBm ($1 \mu\text{A}$ to 1 mA , off centered 5 mm). The conversion gain in the high gain mode is 25 ± 0.2 dB and 1.5 ± 1 dB in the low gain mode. The RF module is also capable of injecting a calibration signal of variable amplitude into any of the four electrodes for calibration purposes. Communication with and control of the RF module is done via the IF module using a two way, RS-485 serial link. The TTL level control signals for the attenuator RF switch and the RF boards are produced on the RF logic board which is located in the RF module. To improve radiation hardness of the system, the RF logic board design was implemented using bipolar logic.

The RF switching, amplification, down conversion and IF amplification were implemented on the RF board. A simplified schematic is shown in Figure 2. In this diagram the X+ channel is being switched through a pair of GaAsFET switches (Mini Circuits, YSWA-2-50DR) to the input of an isolator. At the same time the Calibration switch and the X- switch are connected to double the isolation between the channels. From the output of the isolator, that was used to keep the input impedance constant throughout the dynamic range, the signal passes through a 75 MHz bandwidth crystal filter which rejects unwanted beam induced harmonics. The filter is followed by a pair of switches which allow one to switch in a pair of 11.5 dB amplifiers (Mini Circuits, MAR-6) that provide gain during low ($<100 \mu\text{A}$) current operations. The signal is then down converted to 45 MHz, low pass filtered and amplified. The variable gain IF amplifier (Analog Devices, AD603) was adjusted during the module calibration procedure such that the output gain of all of the RF modules provided 25 dB of conversion gain when operated in the high gain mode. The most difficult part of the design was to reduce the VSWR of the input in all modes of operation to a value below 1.2. This was accomplished by using a line transformer which was further tuned during production by adding capacitive stubs to the input traces located between the RF inputs and the first RF switches. This resulted in VSWR values between 1.03 and 1.19 at all RF inputs.

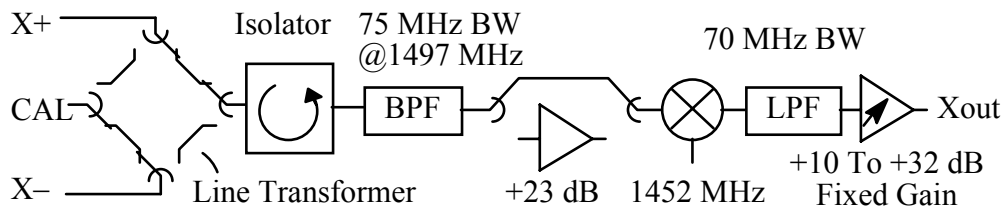


Figure 1. Switched electrode electronics RF chain schematic diagram.

IF Module

The function of the IF module is to amplify the IF signal generated by the RF module and down convert it to a baseband signal that can be digitized with a commercial data acquisition module. A simple schematic drawing is shown in figure 2. The input range of the IF module is -59 dBm to -27 dBm. The first bandpass filter is an LC filter that reduces the broad band noise. It is followed by a pair of variable gain IF amplifiers (AD603) which have 84 dB of dynamic gain control. To further reduce the noise level, the IF bandwidth is limited to 1 MHz using a commercial LC filter. This is followed by a single stage amplifier whose gain is adjusted at the time of calibration. The 45 MHz signal is down converted to base band using a low level video detector (Motorola, MC1330). The base band signal is buffered and filtered by using an 860 kHz low pass filter followed by gated integrating filter which integrates the signal for 2.9 μ s of the 4.2 μ s cycle time. A sample and hold amplifier maintains the signal level at the end of the integration period while the signal is multiplexed with the signal from the Y channel. This produces a series of X+, Y+, X-, Y- signals which are applied to the input of a commercial, 12-bit, high speed data acquisition module (VMIC-3115).

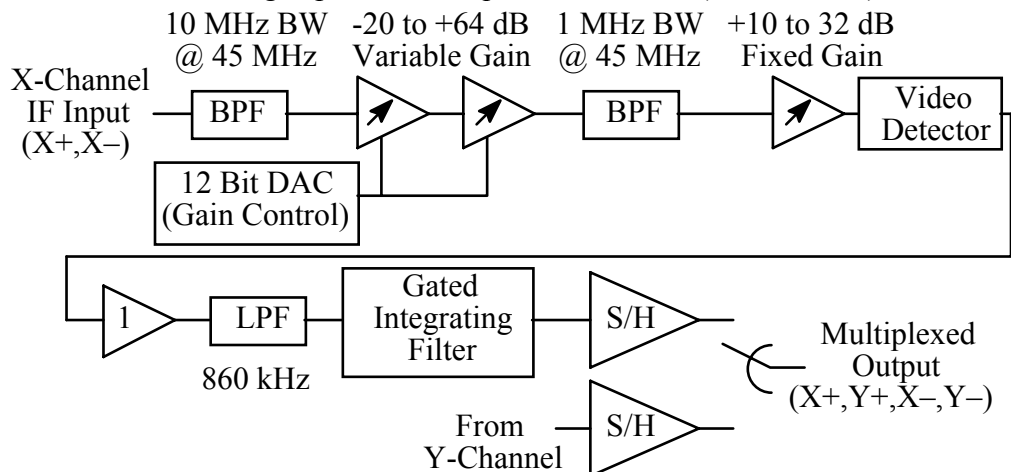


Figure 2. SEE IF module analog chain schematic diagram.

In addition to attention to cross talk and low level noise issues associated with the design and layout of the IF module printed circuit board, there are two subtle details associated with the design of the IF Module. The signal levels at each stage in the IF chain were calculated and the fixed gain IF amplifier was adjusted such that none of the earlier stages saturate prior to reaching the maximum gain. The final critical item was the timing of the gated integrated filter, switch clock, data clock and the multiplexer. Cable transient times and beam delay along the linac (because several channels share the same clock) had to be calculated so that the gated integrating filter was charging only when there was valid data present at the IF module. Additionally, the falling edge of the data clock signal was timed to occur when there were no other digital transitions occurring on the IF card. For this reason, communication between the local VME computer, the timing module, and the IF modules is done using the two bi-

directional data ports on one of the VMIC-3115 modules. The advantage of this is that there was control of all of the logical signals on the IF module which insured that the transitions generated by the bussed control, data and address signals did not interfere with the low level 45 MHz signals.

Timing Module

System timing and synchronization is controlled by the timing module which produces the timing signals for all of the IF modules in a given VME crate, the acquisition clock for the data acquisition modules, the delays required for multipass operation and the pulse count per acquisition trigger. The clock on the timing module was selected such that the system operates at the revolution time of the machine ($4.237 \mu\text{s}$) to within 0.02%. The delay control, which was required for multipass operation, allowed a variable control between 109 ns and $27 \mu\text{s}$ in 109 ns steps. The timing module is a straight forward digital design implemented with a combination of PLDs and discrete logic.

Operational Software

During normal operations the data is synchronously acquired at a 248 kHz rate and processed locally by a Motorola MV162 single board VME computer (68LC040 based). This computer runs a custom-written data acquisition task under VxWorks, which processes the raw digital data into beam position. This task also implements a digital gain control loop so that the video detectors operate in their linear range. The X and Y beam positions that this task computes are passed to an EPICS [7] network database, which also runs on the local computer. From there, the beam position is made available over ethernet to high level applications and displays that run on Unix host computers.

The low level data acquisition task is also set up to acquire calibration data on demand: without beam, the calibration oscillator is turned on and routed to one of the electrodes, and the output signals from the other axis are recorded as a function of IF amplifier setting. This data is used to determine offset between electrodes, due to VSWR mismatch, cable differences, and detector imbalance. Finally, the system can be used to acquire a trace of beam motion for as much as 68 ms at the full 128 kS/s data rate. In one case, five BPM's in one crate have been simul-taneously sampled in this mode, providing complete characterization of the beam properties (current, x , x' , y , y' , E) with a measurement bandwidth of 60 kHz.

LABORATORY RESULTS

Figure 3a shows the beam position as a function of beam current, measured under laboratory conditions. The beam was simulated by using a power splitter with a 4.5 dB attenuator inserted in the X+ line. The input power was varied from -100 dBm to -10 dBm ; the AGC circuit in the IF module was controlled and the

data was acquired using a VMIC-3115 module controlled by a Macintosh computer running LabVIEW®. Approximately 2000 position readings were acquired for each data point on the graphs. The thermal noise and bandwidth of the system limit the low current operation within the specified $\pm 100 \mu\text{m}$ to 400 nA in high gain mode and $5 \mu\text{A}$ in low gain mode where the high and low gain refer to the gain setting in the RF module. Below these values the video detector in the IF module is not capable of reliably locking into the 45 MHz IF signal because of the level of the broad band noise. Figure 3b shows the standard deviation of the position as a function of beam current. This indicates that signal averaging must be employed at currents below $10 \mu\text{A}$ (high gain) and $100 \mu\text{A}$ (low gain) to insure reasonable data. At the high current end of the operations the IF module gains saturate at $125 \mu\text{A}$ and 2.5 mA depending on the gain setting of the RF module.

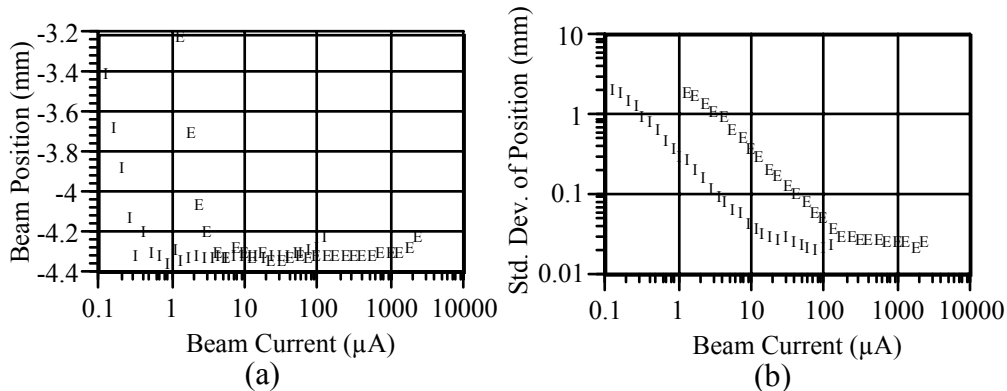


Figure 3. (a) Beam position and (b) standard deviation of beam position as a function of beam current in a laboratory setup which includes a SEE RF module, a SEE IF module and a SEE timing module. An “X” indicates RF module high gain operation and an “O” indicates RF module low gain operation. The data on (b) is position data taken at 124 KS/s .

OPERATIONAL EXPERIENCE

Figure 4 shows the measured beam position as a function of location for seven different currents ranging from 500 nA to $100 \mu\text{A}$. These data were taken by varying the current of a single pass beam in the CEBAF accelerator while maintaining all other machine parameters fixed. 144 readings were averaged for each point shown. Figure 5, is another representation of the same data. In this figure each data point represents the difference between the recorded values and the average of all the points for which the current exceeded $10 \mu\text{A}$ at each machine position. With the exception of 1.7% of the data, the drift of the position as function of beam current is $< 100 \mu\text{m}$ when the beam current is $> 1 \mu\text{A}$. Additionally, only one data point is $> 100 \mu\text{m}$ from the mean value when the current is $> 10 \mu\text{A}$.

Two factors contribute to the uncertainty of the measurements with beam. The first is the number of readings taken. For the laboratory measurements, 2000 readings were averaged for each data point. This becomes more important as the

beam current decreases below 1 μA where the standard deviation of the position readings is greater than 400 μm . The second factor is the uncertainty of the actual beam position stability during the 1 1/2 hours that it took to ramp the current and

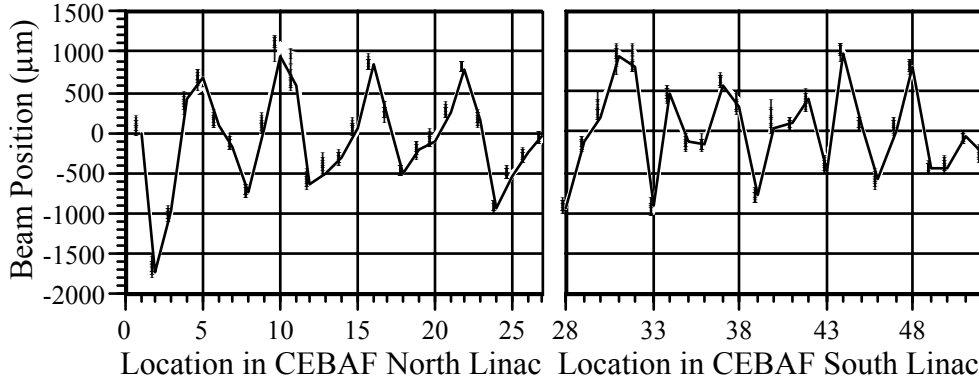


Figure 4. Measured Beam Position as a function of location in the CEBAF linacs for seven different values of beam current between 500 nA and 100 μA .

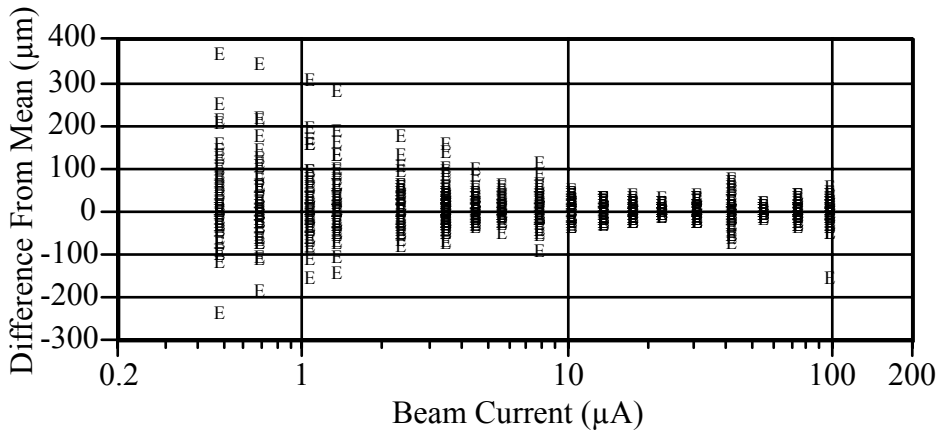


Figure 5. Difference from average of the beam position at each location when the current is $> 10 \mu\text{A}$ as a function of beam current as measured in the CEBAF linacs.

take the measurements. Unfortunately this factor can not be quantified. However, further examination of the data shown figures 4 and 5 indicates that positions 10, 11, 32, 40 and 42 are the only positions in the machine for which the current dependence exceeds $\pm 100 \mu\text{m}$ when the current is greater than 1 μA . The fact that the worst offenders are grouped geographically tends to indicate beam motion.

During normal operations 5 passes of continuous beam are present in the linacs. One machine parameter that has to be controlled is the re-injection properties of the second and subsequent passes (position and angle). The technique that was developed is known as sending a “snake” around the machine. A beam pulse just shorter than the single pass time for the machine, 4.2 μs , is injected into the machine. A beam synchronization pretrigger is applied to the timing module, and the delays on the SEE BPM system are set such that the beam

pulse is captured on each of the five passes without overlap from the previous ones. Each beam pulse is acquired five times as it repeatedly passes through the BPM. Normally the sequence is X1+, X2-, X3+, X4-, X5+ on the first beam pulse followed by X1-, X2+, X3-, X4+, X5- on the subsequent beam pulse, where the number indicates the pass through the accelerator. Thus, data from two successive pulses must be combined before full multipass beam position can be computed. For the SEE system to be operated simultaneously with the 4-channel electronics, installed on the arcs, the actual beam pulse structure consists of a 250 μs pulse followed by a 100 μs pause, followed by a 4.2 μs snake pulse. This is now the normal tune-up mode of operation at CEBAF.

To adjust the delays required for multipass operations, a single pass beam pulse of 4.2 μs is injected into the machine. The delay of each timing module is varied while the outputs of all of the channels in the same VME crate are recorded with the gain control held constant. Figure 6 shows the results of this operation for three of the eight channels in the first VME crate in the machine. Effectively, the charge control signal on the gated integrating filter (2.9 μs) is being convoluted with the beam pulse signal as it arrives at the IF module. The flat top of each of the curves represents the delay time when the integration time occurs coincident with the beam pulse. The difference in the relative position of the flat top is related to the

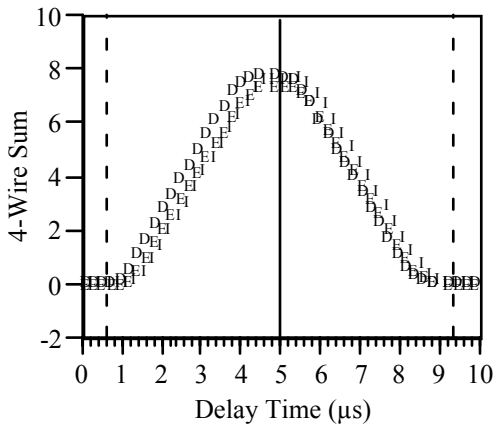


Figure 6. Four-wire sum as a function of delay time for three channels in the same VME crate. The solid line indicates the optimum delay time.

length of the IF module to RF Module cables (30 m to 150 m) and the relative position of the BPM on the beam line. The solid vertical line indicates the optimum delay for that group of channels. The dashed vertical lines indicate the time that next pass beam pulse would be present. Since both the beam pulse and the gated integrator have sharp time-domain cutoffs, cross talk between the passes is kept to a minimum.

Time domain beam position data has been taken using an EPICS based interface. The data shown in figure 7 was taken in a dispersive region of the machine

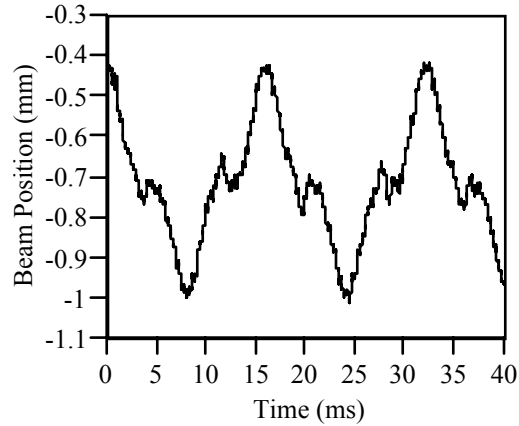


Figure 7. Beam position as a function of time in a dispersive region of the accelerator. The data was filtered using a 20-point running average. [8]

in order to evaluate the need for a beam based fast feedback system. The raw position data, which was acquired at a 124 kHz rate, was filtered using a 20-point running average. The position data represents an energy variation ($\Delta E/E$) of 2×10^{-4} with major harmonic content at 60 Hz, 120 Hz and 180 Hz[8]. To reduce this energy fluctuation, a beam based fast feedback system is being implemented with the SEE BPM electronics.

CONCLUSION

The SEE BPM system installed in the linacs at CEBAF has been presented. The system provides $\pm 100 \mu\text{m}$ accuracy with a position range of $\pm 5 \text{ mm}$ for currents between 400 nA and 2 mA. Beam tests with currents between 500 nA and 100 μA have been presented; they are consistent with laboratory results. The time domain data which has been presented demonstrates the usefulness of the system for the capturing beam motion with an acquisition rate of 124 kHz. Future enhancements to the system include its use in a beam based fast feedback system, increasing the dynamic range, and the lowering of the minimum specified current to levels below 200 nA.

ACKNOWLEDGMENTS

The authors would like to express their appreciation to the machine installation staff who were instrumental in making it possible to bring this system on line 14 months after the beginning of the design process.

REFERENCES

1. Hofler A. S. et al., "Performance of the CEBAF Arc Beam Position Monitors" Proceeding of the Particle Accelerator Conference, Washington DC. 1993, p 2298.
2. J. Cardenas, J-C. Denard "Mesure de Position et d'Intensity" LURE internal report NI/9-75, Orsay 1975
3. Biscardi R., Bittner J.W. "Switched Detector for Beam Position Monitor" Proceeding of the Particle Accelerator Conference, Chicago, Il., 1989, p.1516.
4. Kleman K.J. "High Precision Real Time Beam Position Measurement System" Proceeding of the Particle Accelerator Conference, Chicago, Il., 1989, p.1465
5. Ursic R. et al., "High Stability Beam Position Monitoring of ELETTRA" 1st DIPAC, Montreux Switzerland 1993
6. Barry, W., Nucl Instrum Meth, A301, pp407-416, 1991.
7. Dalesio, L. R., et al., "The EPICS Architecture", ICALEPCS Proceedings, 1991 p. 278.
8. Chowdhary, M., CEBAF, personal communication.



Improvement of the Noise Figure of the CEBAF Switched Electrode Electronics BPM System*

Tom Powers

*Thomas Jefferson National Accelerator Facility,
12000 Jefferson Ave., Newport News, VA 23606*

Abstract. The Continuous Electron Beam Accelerator Facility (CEBAF) is a high-intensity continuous wave electron accelerator for nuclear physics located at Thomas Jefferson National Accelerator Facility. A beam energy of 4 GeV is achieved by recirculating the electron beam five times through two anti-parallel 400 MeV linacs. In the linacs, where there is recirculated beam, the BPM specifications must be met for beam intensities between 1 and 1000 μA . In the transport lines the BPM specifications must be met for beam intensities between 100 nA and 200 μA . To avoid a complete redesign of the existing electronics, we investigated ways to improve the noise figure of the linac BPM switched electrode electronics (SEE) so that they could be used in the transport lines. We found that the out-of-band noise contributed significantly to the overall system noise figure. This paper will focus on the source of the excessive out-of-band noise and how it was reduced. The development, commissioning and operational results of this low noise variant of the linac style SEE BPMs as well as techniques for determining the noise figure of the RF chain will also be presented.

INTRODUCTION

The switched electrode electronics beam position monitor (SEE BPM) system, which was developed and installed in 1993 - 1994, was designed to operate in the CEBAF accelerator linacs where the designed beam intensity range is 1 μA to 1000 μA (1). In most of the remainder of the machine, which is collectively known as the transport lines, the nominal beam intensity range is between 100 nA and 200 μA . The exception is the Hall B transport line where beam intensities as low as 200 pA are used. Because these beam intensities are below the limits of the existing BPM systems used at CEBAF, two new systems have been developed. The system which is used at the very low beam intensities, known as the 1 nA beam position monitoring system, is a cavity based system which makes use of lock-in amplifiers to provide synchronous detection of the position sensitive signals. This system is fully described in (2). The second system, which will be described in this paper, is known as the transport line switched electrode electronics system (TL-SEE). It is a low noise variant of the linac style system which makes use of GaAs switches and variable gain amplifiers to cover the required dynamic range while maintaining a precise gain balance between the plus and minus signals of the X and Y electrode planes.

SYSTEM PERFORMANCE

The system performance for the linac style and transport line style SEE BPM system is summarized in Table 1. The dynamic range is defined as the range of currents for which the system operates within all other specified limits. The lower end of the dynamic range is limited by thermal noise and the detectivity of the IF down conversion circuit. The high end is limited by signal compression in the electronics.

*Supported by DOE Contract #DE-AC05-84ER40150

TABLE 1. Summary of linac style and transport line style performance specifications

	Linac Style	Transport Line Style
Dynamic range	700 nA - 2000 μ A	70 nA - 200 μ A
Nominal measuring rate out of control system	1 meas./s	1 meas./s
Beam position range	$ x , y \leq 5$ mm	$ x , y \leq 5$ mm
Resolution (rms fluct. at nominal meas. rate)	≤ 0.1 mm	≤ 0.1 mm
Current dependence	≤ 0.1 mm	≤ 0.1 mm
Multipass capability	"snake" pulse	Not required
IF bandwidth	1 MHz	50 kHz
Analog bandwidth	70 kHz	7 kHz
Maximum measurement rate	114 kS/s	7.1 kS/s

SYSTEM DESCRIPTION

Both types of SEE systems use VME based IF, acquisition, and control modules. The VME crates are located in the service buildings approximately 10 meters above the beam line. Each channel consists of a BPM detector, an RF module located in the tunnel and an IF module located in the VME crate. The beamline sensor has four wire-type stripline antennas previously described (3). Each pair of opposing electrodes is time-domain multiplexed into one signal conditioning chain at the front end of the RF module (X+X-X+X-... and Y+Y-Y+Y-...). This is done to insure a balanced gain independent of gain variations in the remainder of the system. These signals are amplified and down converted to 45 MHz before transmission to the IF module. In the IF module, the signal is amplified using a three stage amplifier which has a digitally controlled gain with a dynamic range of 84 dB. The signal is filtered, then down converted to base band, filtered again and further multiplexed before it is transmitted to a commercial data acquisition module as X+Y+X-Y-X+Y+... data. Each crate has a timing module which is used to synchronize the system to the accelerator and to generate specific timing signals required by the IF, and RF modules. The VME crate also contains three commercial data acquisition modules and a single board microcomputer which are used to acquire and process the position signals prior to transmitting them to the machine control system.

The system has two fundamental software interfaces. The first is a once per second average position readout which provides the average position and its rms noise to the machine operators. The second is a beam oscilloscope program which provides time domain and frequency domain measurements of the beam position and intensity modulation at any location of the machine. Additionally, as shown in Figure 1, the program provides a measure of energy "jitter" based on beam position readings in any of 5

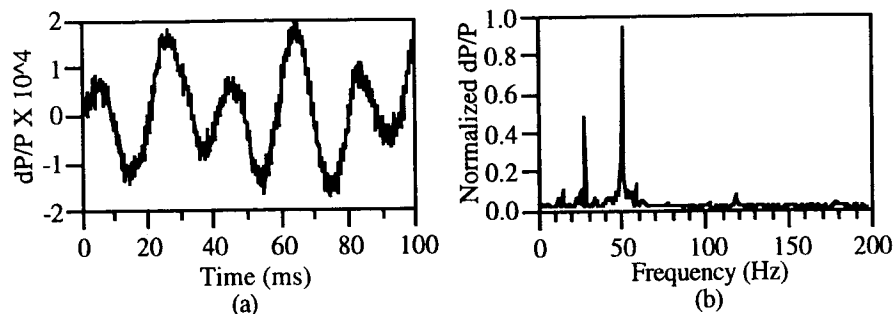


Figure 1. (a) Time domain and (b) frequency domain plots of the energy "jitter" in the Hall C transport line. The 50 Hz and 29 Hz frequency content was due to an SRF cavity with an open phase control loop.

different high dispersion regions of the accelerator. The measurement shown in Figure 1 was made using 5 transport line BPMs whose data was acquired synchronously and processed off line using machine optics information from the CEBAF model server (4). This energy modulation was due to a problem with the phase control loop of one of the 330 superconducting cavities which are the accelerating elements at CEBAF. The problem was quickly rectified once it was identified by the BPM system.

BACKGROUND ON NOISE FIGURE CALCULATIONS

The noise factor of a device is the signal to noise ratio at the output of the device divided by the signal to noise ratio at the input. The noise figure is the noise factor expressed in units of dB. The noise figure is the specification that is normally provided in the component data sheet. One of the standard ways to define the noise factor (F) and noise figure (NF) is:

$$F = \frac{S_i/N_i}{S_o/N_o} = \frac{N_a + kT_oBG_a}{kT_oBG_a} \quad (1)$$

$$NF = 10 * \log(F) \quad (2)$$

Here N_a is the noise power introduced by the device, G_a is the power gain of the device, T_o is 290 K, B is the bandwidth of the system, and k is Boltzmann's constant. Typical noise figures for inexpensive room temperature amplifiers are 1.5 to 10 dB. Amplifiers with noise figures as low as 0.9 dB are commercially available. The noise factor of a passive two port device ($G_a < 1$), which does not contain noise sources other than thermal noise, is equal to the loss of the device, $L = 1/G_a$.

When two or more devices are cascaded, including passive devices, the noise factor for the network is given by the following equation:

$$F = F_1 + \frac{F_2 - 1}{G_1} + \frac{F_3 - 1}{G_1G_2} + \dots \quad (3)$$

Here F_1 , F_2 and F_3 are the noise factors for the first, second and third stages respectively and G_1 , G_2 , and G_3 are the available gains of the first second and third stages respectively. Thus once the first gain stage is accomplished the noise figure contributions to the overall noise figure by subsequent devices is reduced. This is the reason that the most important noise figure is that of the first stage amplifier and that the passive devices before the first amplifier stage should avoided if possible. However, if the front end amplifier gain is not high enough, additional losses may be such that subsequent devices may contribute significantly to the overall noise figure.

There are four contributions to the noise figure when a mixer is used as a down converter (5). The first is equal to the conversion loss of the mixer. The second is the effect of the local oscillator phase noise. The third is the noise generated by the electronic devices, (i.e., FETs for square law mixers and diodes for typical switching-mode mixers). Typically the "electronic" noise adds one or two dB to the noise figure of the circuit. The fourth contribution is the noise at the image frequency of the RF signal. Consider the signal shown in Figure 2. If there is equal noise power at the image frequency, the output noise power at the IF frequency is equal to the sum of the noise power at the signal frequency plus that at the image frequency. This image frequency noise adds 3 dB to the system noise figure independent of the gain of the previous stages. In this case the noise power is added because the two noise signals are uncorrelated.

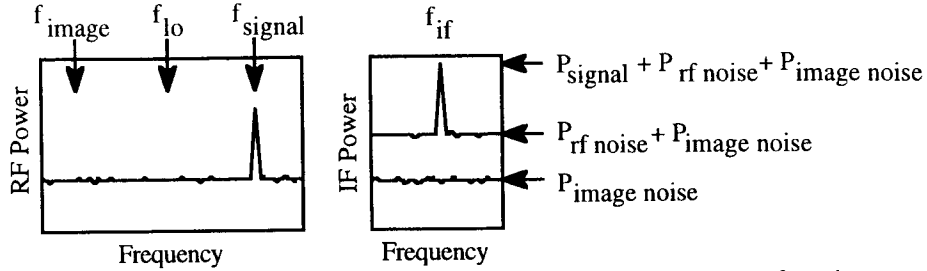


Figure 2. Contribution of image noise to IF noise at the output of a mixer.

Measurement Techniques

There are several ways to measure the noise figure of a device or system. The first is to plot the output noise power with a 50 ohm source impedance at different temperatures (typically 300 K and 77 K).⁽⁶⁾ The P-intercept of a straight line plot of measured output power as a function of temperature is the value of the noise power N_a of the device under test. The second approach is to use a calibrated noise source, a low noise amplifier (LNA) and noise figure meter, or spectrum analyzer with a noise figure personality module. In this technique, the spectral characteristics of the noise source and LNA are measured; the device under test (DUT) is inserted between them; and the instrument calculates the gain and noise figure of the DUT. The third method requires an LNA, a spectrum analyzer and a 50 ohm termination. In the latter two techniques the LNA is used to increase the sensitivity of the measuring instrument in order to increase the measured noise voltage above the noise floor of the instrument. The last technique has the added advantage that “man made” signal sources become apparent when the measurement is being made and one may make compensations while the first two systems provide only a noise figure at specific frequencies.

The noise factor of an amplifier can also be written as:

$$F = \frac{P}{kTBG} \quad (4)$$

Here P is the output noise power with the input terminated, T is the absolute temperature of the termination, k is Boltzmann’s constant, and G is the amplifier gain. For a 50 ohm system with a preamplifier inserted between the DUT and the spectrum analyzer this equation may be written as:

$$NF(\text{dB}) = 10 \log \frac{V^2}{R} - 10 \log B - 10 \log (G_a + G_p) - 10 \log kT \quad (5)$$

Here G_p is the gain of the preamplifier, V is the rms voltage reading, and B is the measurement bandwidth. The reading is done using the voltage scale in order to increase the resolution. This equation can be further reduced to:

$$NF(\text{dB}) = 20 \log V - 10 \log BW - 10 \log (G_a + G_p) + 187.27 \text{ dB} \quad (6)$$

Here BW is the 3 dB bandwidth of the spectrum analyzer, and 187.27 is a result of the sum of four numbers: $-10 \log 50 \text{ ohms}$; $-10 \log kT$; $-10 \log 1.2$ (an approximate correction factor to go from noise power bandwidth to Gaussian 3 dB bandwidth); and $+1.05 \text{ dB}$ (detector correction factor)⁽⁷⁾. In order to make accurate voltage measurements, strong video averaging is applied with typical averaging factors of 1000. Additionally, one must be careful to keep the peak signals, without averaging, below the saturation levels of the instrument by adjusting the vertical scale with averaging off and turning averaging on before making a measurement.

IMPROVEMENT TO THE NOISE CHARACTERISTICS

Four fundamental changes were made to the system to improve the low current operations. Three changes were made to the RF module which improved the noise characteristics at lower beam intensity by 8 dB or a factor of 2.5. Improvements were made to the IF module which increased the sensitivity by 13 dB or an additional factor of 4.4 lower in beam intensity. These improvements should have extended the dynamic range at low currents by a factor of 11 from 700 nA to 64 nA. As will be shown, the actual increase in sensitivity was only a factor of 10 or down to 70 nA.

IF Module Improvements

The function of the IF module is to amplify the IF signal provided by the RF module and down convert it to a baseband signal that can be digitized with a commercial ADC module. A simple schematic diagram of the linac style IF module is shown in Figure 3. A detailed description of the function of the linac style IF module may be found in (1). Three changes were made to improve the noise characteristics of the system: the 1 MHz BW @ 45 MHz LC filter was changed to a 50 kHz BW @ 45 MHz crystal filter; the 860 kHz low pass filter was changed to a 100 kHz low pass filter; and the integration time of the gated integrated filter was changed from 3.2 μ s to 30 μ s. This last change was done because the switching clock frequency was reduced from 248 kHz to 14.2 kHz so that the plus-to-minus modulated IF signal is sufficiently settled before the integration process is initiated. The settling time for the 1 MHz BW filter is 500 ns while the settling time of the 50 kHz BW filter is 25 μ s. The changes which were made to the baseband section of the IF module improved the noise characteristics of the output signal while the low current limitations of the system remained the ability of the video detector to lock on the IF frequency in the presence of noise. Thus the only improvement which impacted the low current limit was the reduction of the bandwidth of the 45 MHz band pass filter.

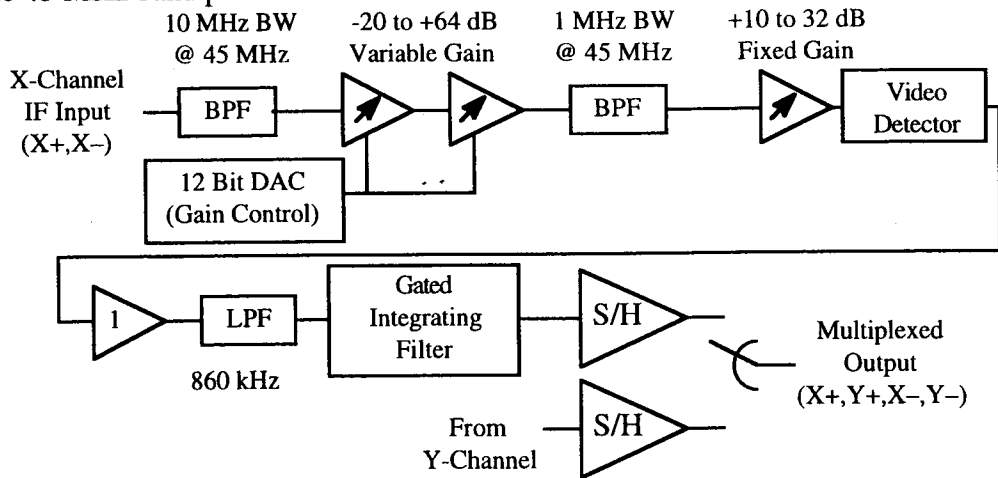


Figure 3. Simplified schematic diagram of the linac style IF module.

RF Module Improvements

A detailed functional description of the RF module can be found in (1). The RF chains for the two systems are shown in Figure 4. Three changes were made to the linac style system in order to improve the low current performance. The first change is that the 1497 MHz band pass filter was relocated to just before the mixer in order to improve the

overall noise figure by 6.8 dB. For the second change, the two-stage RF amplifier was changed from two MAR-6 amplifiers to one MAR-6 amplifier and one ERA-3 amplifier. This increased the RF gain from 23 dB to 32 dB without degrading the noise figure. Thirdly, the gain was adjusted on the output stage IF amplifier to provide an overall gain of 38 dB vice the 25 dB setting used in the linac style system. This, along with increased overall gain prior to this section, had the additional benefit of decreasing the overall noise figure by another 1.5 dB. The range of input power levels for the linac style RF module is -77 dBm to -4 dBm, which equates to an intensity range of 700 nA to 2 mA. The range of inputs for the Tline style RF module is -97 dBm to -27 dBm, which equates to an intensity range of 70 nA to 200 μ A.

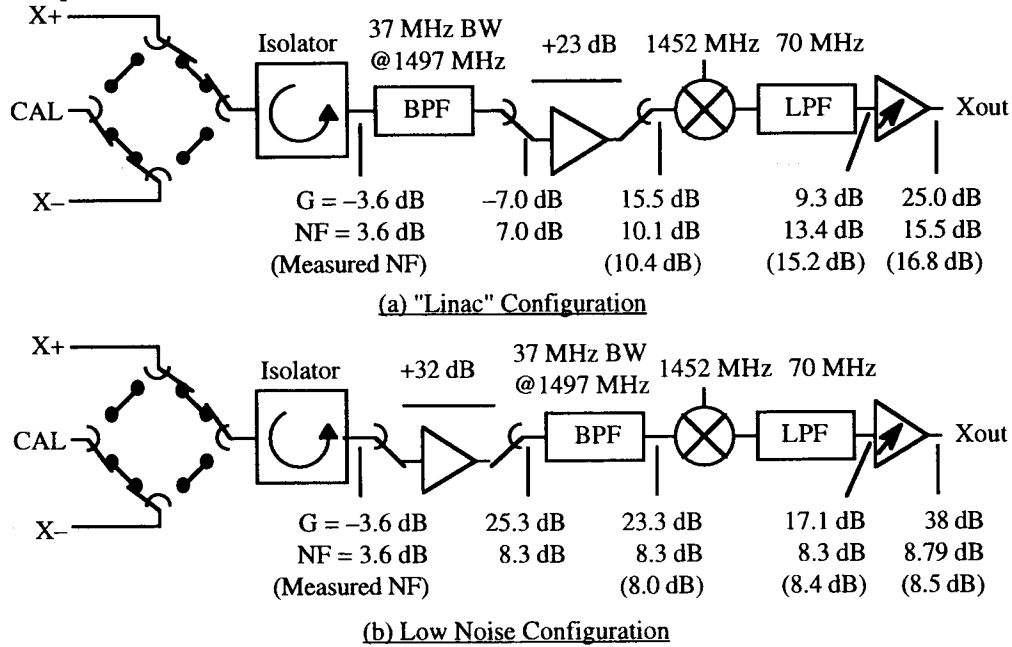


Figure 4. Switched electrode electronics RF chain schematic diagrams showing the linac configuration and the low noise, transport line, configuration. The noise figures within parentheses are measured values while the other noise figures, as well as the gains (G), were calculated based on typical measured values.

Relocating the filter had two expected and one unexpected effects. The first effect is the reduction of the overall noise figure by 2 dB (the in-band attenuation of the filter) because the filter was moved to a point after the initial gain stage. Thus the contribution to the noise figure due to the loss was reduced by $(F_{\text{filter}} - 1)/G_i$ where G_i is the combined gain of the switches, the circulator and the two-stage amplifier. The second effect was the reduction of the overall noise figure by 3 dB because the filter rejected the noise at the image frequency of 1542 MHz. The third effect was one of the two more subtle improvements associated with the changes.

When performing the initial system noise figure measurements, the circuit, at the mixer output, had 2 dB of unaccounted for noise figure. Figure 5 shows the normalized noise power as a function of frequency at the input of the mixer for both circuits. The noise power at the image frequency for the circuit with the filter prior to the amplifier is 1.8 times the power level at the signal frequency. By adding this to the in-band noise you would get a noise figure increase of 5 dB vice the 3 dB that is expected from an SSB down conversion with uniform noise in both the image and signal frequency bands. Further investigation of the characteristics of the band pass filter indicated that the filter

does reject signals at the image frequency by more than 30 dB. However, the output port of the filter is almost totally reflective at the image frequency. A reflective source will reflect any noise power coming out of the input port of the amplifier circuit back into the amplifier for amplification. The second subtlety is the noise figure of the AD603 variable gain amplifier which is the last stage of the circuits shown in Figure 4. The first page of the specification sheet indicates that the input noise spectral density is $1.3 \text{ nV}/\sqrt{\text{Hz}}$, which corresponds to a noise figure of 9.5 dB for the amplifier bandwidth of 50 MHz and a gain of 32 dB. However, the variable gain function of this amplifier was implemented by an R-2R ladder network followed by a fixed gain amplifier. This ladder network is in effect a voltage controlled attenuator. Thus as the overall gain is reduced by 10 dB the noise figure of the AD603 increases by 10 dB. By increasing the gain of the IF stage from 18 dB to 23 dB, the noise figure of the IF stage was reduced from 21 dB to 16 dB and the overall noise figure of the RF module was reduced by 0.85 dB.

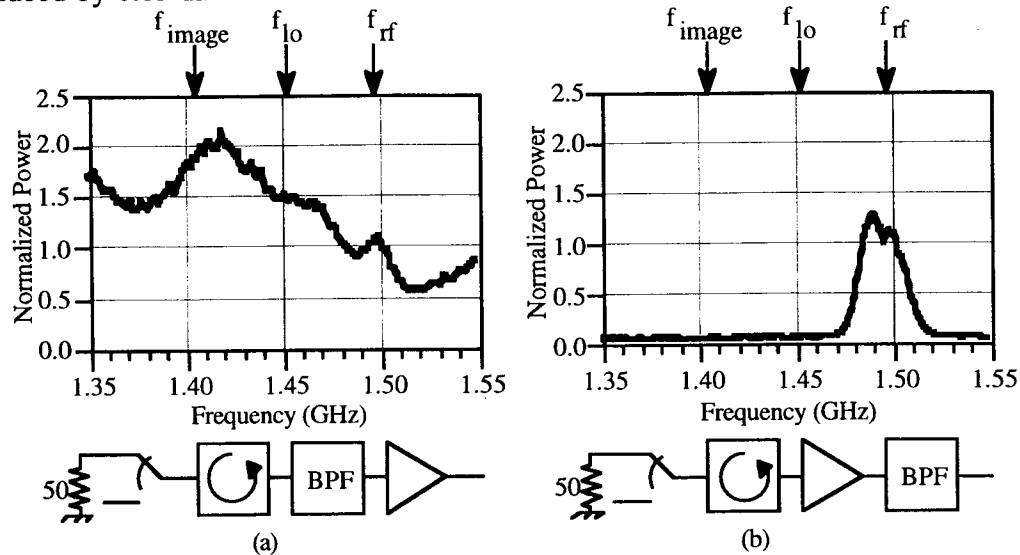


Figure 5. Normalized noise power as a function of frequency for two different circuit topologies. The first is the topology used in the linac style system while the second is that used in the transport line system.

RESULTS

During the production testing the low current capability of all of the RF modules was determined. For practical reasons, this low current limit is defined by the rms value of the position noise. As is shown in Figure 6, the low current beam position is valid (within $200 \mu\text{m}$ of the maximum value) when the rms value of the instantaneous beam position readings is less than 1 mm. Further analysis of the production test data shows that position readings at the minimum current value on all of the channels used to generate Figure 6(b) were within $\pm 120 \mu\text{m}$ of the maximum value. An additional 12% reduction in beam current was required before any of the modules varied by more than $200 \mu\text{m}$ from the maximum position. Figure 7 shows histograms of the results of this analysis. Only two of the transport line modules which were analyzed had a measured low current limit above 70 nA while most of the modules made it down to 60 nA. This data is shown in Figure 7(b). An analysis of the production data from the linac style modules indicates that the low current limit for this style is 700 nA with most modules making it down to 550 nA. This data is shown in Figure 7(a).

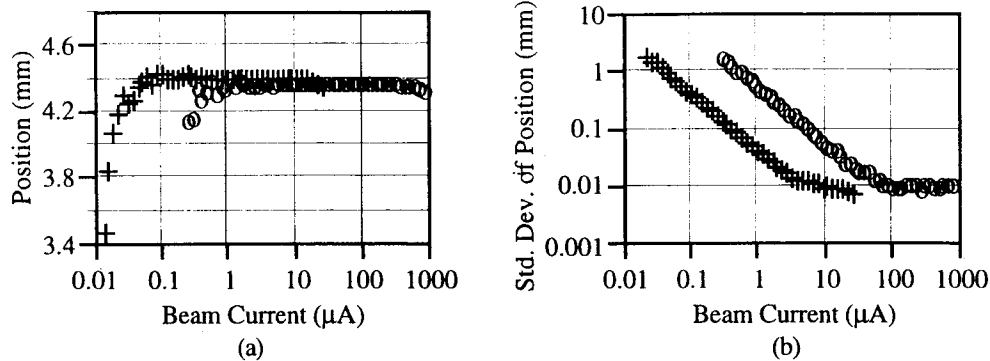


Figure 6. Typical plots of (a) beam position as a function of beam intensity and (b) standard deviation of the $140 \mu\text{s}$ beam position readings as a function of beam intensity. Both sets of data were taken using transport style electronics in the laboratory. The data indicated with a “+” is for the high gain setting and an “o” is for the low gain setting.

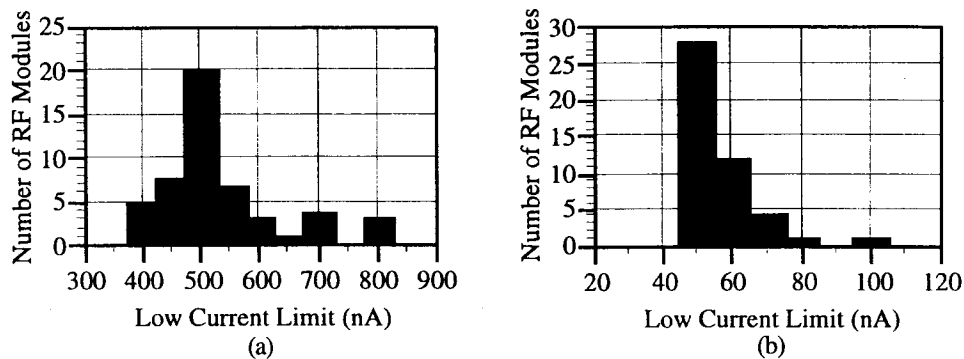


Figure 7. Low current limitations of (a) 48 linac style RF modules and (b) 46 transport line RF modules as measured during production testing.

CONCLUSION

A description of how the noise figure is measured as well as the basic formula for calculation of the noise figure of a multi-stage system have been presented. Application of these principles to improve the low current operation of the SEE BPM system was also described. By changing the bandwidth of the IF section, the judicious swapping of circuit elements in the RF section, and the adjustment of the gains in the RF module, the low current capabilities have been improved from 700 nA to below 70 nA. This was accomplished without doing a major redesign of the system packaging, digital interface or software.

REFERENCES

1. Powers, T., et al., “Design, Commissioning and Operational Results of Wide Dynamic Range BPM Switched Electronics. *Proceedings of the Seventh Beam Instrumentation Workshop*, p 257.
2. Piller, C., et al., “1 nA Beam Position Monitor”, presented at this conference.
3. Barry, W., *Nucl Instrum Meth*, A301, pp#407-416, 1991.
4. Van Zeijts, J., et al., “Integrated On-Line Accelerator Modeling at CEBAF”, *Proceedings of the 1995 Particle Accelerator Conference*, p 2181.
5. Hayward, W., *Introduction to Radio Frequency Design*, American Radio Relay League, Inc. 1994, pp. 202 - 246.
6. Gardiol, F. E., *Introduction to Microwaves*, Artech House, Inc. 1984, p. 362
7. “Spectrum Analysis, . . . Noise Analysis” Hewlett Packard Application note 150-4, April 1974.

Performance of the CEBAF Arc Beam Position Monitors*

A. S. Hoffer, B. A. Bowling, C. S. Higgins, P. K. Kloeppe, G. A. Krafft, K. L. Mahoney
The Continuous Electron Beam Accelerator Facility
12000 Jefferson Ave., Newport News, VA 23606

Abstract

The first three quarters of the first CEBAF arc have been instrumented with beam position monitors. Thirty-seven monitors (of 450) have been installed and their noise measured. Resolution of 100 μm was obtained at the lowest operating current of 1 μA . The update time of the system is 1 sec, limited by computer interfacing, with a potential bandwidth of greater than 10 kHz.

I. INTRODUCTION

The basic requirements for the beam position monitor system are dictated by the properties of the beam. In the accelerator arcs, the range of currents that should be accurately detected is from 1 μA to 200 μA . The beam size in these regions is approximately 100 μm rms. Therefore a system with 100 μm position resolution is appropriate. The BPMs should be useful both in CW mode, the standard operational mode for CEBAF, and in a pulsed low-power tune-up mode in which, for machine safety, the beam pulses are limited to about 100 μsec . The BPMs provide primary signals for feedback stabilization purposes.

A basic schematic of the system is shown in Fig. 1 [1]. Starting on the beam line, the fundamental frequency of the beam is induced on each of four BPM wires and transmitted to a B0005 chassis, better known as the arc tunnel electronics. Here the signal is amplified and down-converted to 1 MHz for transmission to detection circuitry in the service buildings upstairs. Each of the 1 MHz signals from the B0005 box is sent to a separate channel of a B0007 board resident in a CAMAC crate upstairs. In the B0007 board, the amplitude of the 1 MHz signal is detected and digitized. The digitized voltage levels are then conveyed to the computer where the beam position is computed.

If there were no errors in the system, and if X_{\pm} and Y_{\pm} were proportional to the amplitude of the beam generated signal on each wire, the beam position before rotation could be calculated as

$$X' = k \frac{X_+ - X_-}{X_+ + X_-},$$

and likewise for Y' , where k is the sensitivity of the BPM at 1500 MHz.

Because of errors in the system, two software corrections are made. The first deals with the fact that the amplitude gains in the different channels might be different.

The second deals with the offsets that exist in the amplitude detector. The modified computation of the unrotated positions is

$$X' = k \frac{(X_+ - X_{\text{off}+}) - \alpha_X(X_- - X_{\text{off}-})}{(X_+ - X_{\text{off}+}) + \alpha_X(X_- - X_{\text{off}-})},$$

and likewise for Y' , where α_X , α_Y , $X_{\text{off}\pm}$, and $Y_{\text{off}\pm}$ are measured by the automatic calibration circuitry as follows:

- Using the zero wires facility in the software, measure the offset voltages $X_{\text{off}\pm}$ and $Y_{\text{off}\pm}$ with both the beam and calibration signal off,
- calibrate the X channels with a calibration signal on y_- , and
- calibrate the Y channels with a calibration signal on z_- .

The word "calibrate" means to find the relative gain ratios α_X and α_Y for the X and Y channels respectively. This is done by measuring the amplitude ratio when the beam is off and the calibration signal is on:

$$\alpha_X = \frac{X_+ - X_{\text{off}+}}{X_- - X_{\text{off}-}},$$

and likewise for α_Y .

The beam position, after rotation by 45°, is

$$\begin{pmatrix} X \\ Y \end{pmatrix} = \frac{1}{\sqrt{2}} \begin{pmatrix} 1 & -1 \\ 1 & 1 \end{pmatrix} \left[\begin{pmatrix} X' \\ Y' \end{pmatrix} - \begin{pmatrix} X'_{\text{off}} \\ Y'_{\text{off}} \end{pmatrix} \right],$$

where the offsets X'_{off} and Y'_{off} are used to save particular orbits as discussed below.

II. HARDWARE DESCRIPTION

A. Mechanical

The beam position monitors that are used in the CEBAF arcs are two models of the same basic design. They consist of four thin-wire quarter-wave pickup antennas, symmetrically placed at the corners of a square that is perpendicular to the beam and centered on the beam axis [2]. The pickups are parallel to the beam. The monitors in the first of the five beam passes must be accommodated to a larger beam pipe than the others, nominally 4.7 cm (the M20 monitor) as compared with 3.5 cm (the M15 monitor). The diameter of the outer shell is fixed by the requirement that the impedance be 200 Ω . Up to the present, most beam tests have been performed with M20 monitors; there is no evidence that the M15 monitors give substantially different results.

The pickup wires are approximately positioned in the manufacturing process. They are then individually positioned with the aid of an optical comparator to within 75 μm . When this process is completed, their electrical response is individually measured with a network analyzer to ensure that it is within acceptable limits. The monitors are

*Supported by U.S.DOE contract DE-AC05-84ER40150.

then cleaned and slow-baked, and finally are leak-tested. If accepted, they are released to be installed on the accelerator beamline. The BPM sensitivity k is measured for every monitor; the values usually are within 1% of 18.5 mm.

B. Electrical

The electronics portion of the arc BPM system is composed of a heterodyne front-end preamplifier located in the tunnel enclosure and a synchronous amplitude detector located in the service buildings.

The front-end B0005 electronics amplifies, and then downconverts each of the four position inputs from 1.5 GHz to 1 MHz. The 1 MHz signals are buffered and sent upstairs to be detected. An oscillator used in the calibration and testing of the BPM system is included in the front-end electronics; it is activated only during the calibration sequence. If both channels are working correctly the relative gain ratio should be approximately 1.

The B0007 detector card includes a programmable gain amplifier, synchronous detector, and analog-to-digital converter on each channel. The detection and conversion may be either internally (CW mode) or externally (pulse mode) triggered, selectable by the operator. The minimum detectable pulse width is governed by the synchronous detector and is on the order of 25 μ sec.

The synchronous detector system is used to provide an amplitude-detected signal for each channel. The instantaneous dynamic range of the detected signal is governed by two factors. First, the detector has a minimum threshold below which it cannot phase lock the incoming signal. Second, the detected signal is digitized using an 8-bit analog-to-digital converter which limits the signal range to 256 states. For this reason a programmable gain amplifier is included in the detector front end. The gain, adjustable over a 30 dB range, is set according to the expected value of the operating current of the accelerator.

Because the arc BPM is a linear difference-over-sum system, special attention is given to ensure sufficient dynamic range and signal-to-noise ratio in the preamplifier and detector subsystems. The CEBAF peak beam current ranges from 1 to 200 μ A, giving a signal level between -73 and -27 dBm on center. Care is taken to ensure sufficient signal-to-noise ratio through the detector. The front-end preamplifier establishes the system noise figure at approximately 4 dB.

III. SOFTWARE DESCRIPTION

The BPM software system, part of the TACL [3,4] control system, consists of an operator interface and software controls. The interface is comprised of three types of TACL display pages running on console computers. The software controls reside in user functions in TACL logic processed on front-end computers attached to CAMAC crates. Communication between the operator in the control room and the B0007 cards in CAMAC crates in the service buildings is managed by the software system.

The basic software organization is that one BPM user function accesses one B0007 card, but display pages may provide monitor and control capabilities for one or more BPMs. Various BPM operating modes, for example the calibration mode, are requested and monitored by the operator via display pages, and these requests are interpreted and passed by logic to the selected user functions. All signal and position information generated by the user function is calculated using ADC wire data acquired by logic from the B0007 card. Other CAMAC interactions required to initiate and terminate BPM operating modes are handled by the user function. The user function converts and calculates all of the data from the BPMs on the display pages.

The information from the BPM system is displayed in the control room in three ways. Beamline screens are used in daily operations and provide the relative position of the BPM on the beamline, the device name, and the calculated beam position in millimeters or the BPM status. Second, test screens provide the operational controls for the BPMs and display system information such as read-backs for wire signal values, position and wire offsets, calibration constants, and approximate beam current. Finally, "Red October" charts display all of the BPM positions in individual sonar-like displays.

During normal operations the user function converts filtered ADC wire values to positions. The normal mode of filtering collects one set of values at the same cycle rate as logic (3 to 8 Hz) and averages them continuously, giving position data that lag the machine state by 20 sec without degrading overall performance. This lag can be reduced to less than a second at the expense of front-end performance if logic reads the BPM crate many times per logic cycle and provides an averaged ADC value to the BPM user function. This second mode of filtering results in a reduction of overall front-end performance by a factor of three. Such filtering modes can be combined to achieve the best tracking response while minimizing the impact on performance. The normal filter mode can be applied globally to all the BPMs in the machine or can be specified for a subset of BPM modules. The CAMAC averaging scheme is specifically invoked for subsets of BPM modules. Because of the performance cost, it should be reserved for situations where tracking response time is a concern, as with automated optics setup software [5,6].

One of the capabilities of the user function is to define a "golden orbit" or position offset. The BPM electronics pick up noise from neighboring RF cavities and power sources as well as the beam signal, resulting in false or offset position readings. This can be eliminated by establishing an acceptable beam orbit and requesting the user functions to use the current positions as the zero reference. Once these offsets are recorded, they are subtracted from the calculated positions until a new "golden orbit" is defined. Currently, this option is used most with automated orbit correction algorithms which attempt to center positions in the BPMs [5].

During the recent series of pre-commissioning tests, the BPMs were most useful in initial manual beam threading efforts. In the user function the wire currents are summed together, providing an approximate beam current seen by the BPM. By watching the beam current values and the position readback on the test display screens, it is easy to determine whether or not the beam is passing through a specific BPM.

IV. RESULTS

Initial tests of the tunnel electronics uncovered two problems which have subsequently been remedied. The first was that the components selected for the microwave front-end amplifier were not ideally suited for 1497 MHz operation. Second, the tunnel electronics were susceptible to radiated interference from external sources. Both problems were addressed by redesigning the tunnel electronics using surface-mount technology. Initial tests of the redesigned board show measurable improvements in gain, noise immunity, and stability.

In Fig. 2, a graph of beam position as a function of time demonstrates the ability of the monitors to respond to weak currents. The jitter in position is the result of both electronics noise and actual beam motion. It is in any case less than about 0.1 mm rms at $0.5 \mu\text{A}$, and is smaller at high currents. For example, at $10 \mu\text{A}$ (not shown), the jitter is only about one-fourth as large. Whether the beam is diagnosed in CW or pulsed mode, the position fluctuation after averaging is the same.

Thirty seven complete systems were installed and operated simultaneously, extending throughout the spreader

and the first three quarters of the east arc. In normal operations, the software provided quick and reliable information, especially when the block reads were successfully implemented. The BPM test screens, through the calibration options, provided especially useful diagnosis of hardware problems.

V. CONCLUSIONS

The CEBAF arc beam position monitors have been successfully used to diagnose the CEBAF beam in the first spreader and east arc of the CEBAF electron accelerator. The monitors are the only means of steering in a large section of the machine, and this section of the machine was traversed the first time with little additional difficulty. They have operated under a wide dynamic range in addition to the standard tune-up setting of about $10 \mu\text{A}$ beam current. Experiments reported in several other papers in this conference required functional BPMs. In particular, the automatic steering routines [5], east arc commissioning [6], and the energy correction hardware/software [7] relied on the arc BPMs.

VI. REFERENCES

- [1] W. Barry, J. Heefner, and J. Perry, *Proc. 1990 Beam Instrumentation Conference*.
- [2] W. Barry, *Nucl Instrum Meth A301*, 407-416 (1991).
- [3] R. Bork *et al.*, *Proc. 1989 Part. Accel. Conf.*
- [4] M. Bickley, and J. Kewisch, these proceedings.
- [5] B. Bowling *et al.*, these proceedings.
- [6] Y. Chao *et al.*, these proceedings.
- [7] G. Krafft *et al.*, these proceedings.

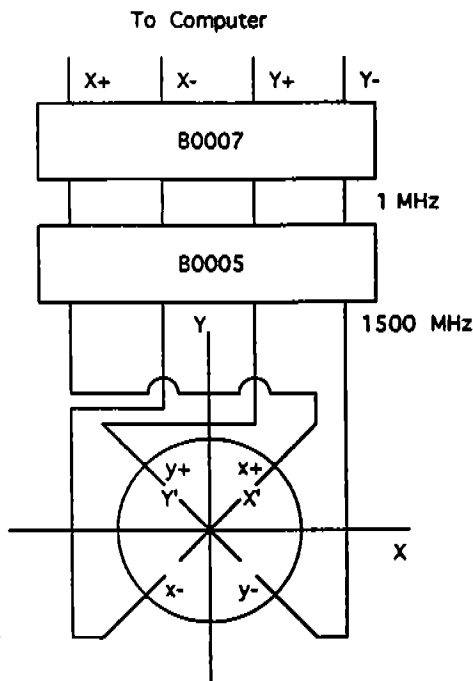


Figure 1. Block diagram of BPM electronics.

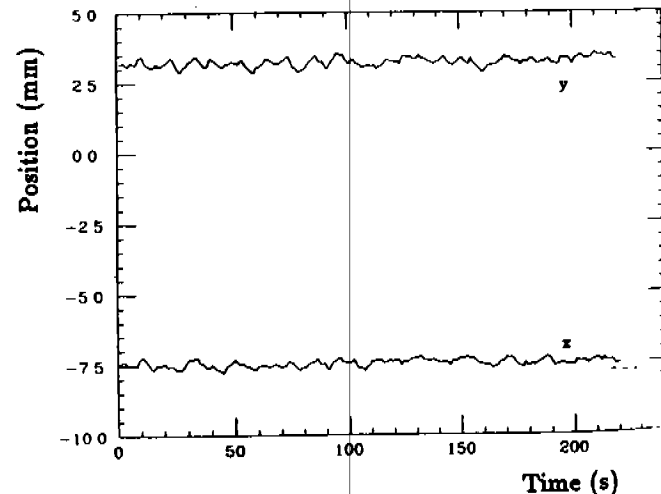


Figure 2. Position seen at $0.5 \mu\text{A}$.



CEBAF-TN-93-004
 Geoffrey Krafft
 Alicia Hofler
 1/12/93

How the Linac Beam Position Monitors "Work"

At present, there is great confusion about employing the linac beam position monitors in beam dynamics measurements. Therefore, it seems useful to summarize what can and cannot be done with the present system. In this note, the present status and utility of the linac beam position monitors is described.

How Should the Linac BPMs Work?

The current linac monitors, which are of an inductive loop type, were designed to operate at 100 MHz. The detected signal was to originate from a current modulation on the CEBAF electron beam. The modulation was to be of a special type, where sequences having pseudorandom character could be used to allow one to separate the coordinates of the separate beam passes by electronic means.

Due to the difficulty of current modulating the beam at 100 MHz without emittance growth, it was decided to investigate again using the 1500 MHz fundamental frequency as the carrier. This choice has two attendant difficulties: the BPM pick-up response is down by more than an order of magnitude at 1500 MHz and any 1500 MHz signals not originating on the beam can be a noise source in the measurements.

The system, as installed on several linac monitors at present, is shown in Figure 1. The idea is to use arc monitor detection electronics with the linac monitors, and to postpone multipass detection until it is necessary later. Starting on the beam line, the beam fundamental frequency is picked up on each of the BPM wires and transmitted to an arc B0005 box, better known as the arc tunnel electronics. Here the signal is amplified and downconverted to 1 MHz for transmission to detection circuitry in the service buildings upstairs. Each of the 1 MHz signals from the B0005 box is sent to a separate channel of a B0007 board resident in a CAMAC crate upstairs. In the B0007 board, the amplitude of the 1 MHz signal is detected and digitized. The digitized voltage levels are then conveyed to the computer where the beam position is computed.

If there were no errors in the system, the beam position could be computed as follows. If X_{\pm} and Y_{\pm} are proportional to the amplitude of the beam generated signal, and if

$$X' = k \frac{X_+ - X_-}{X_+ + X_-}$$

and

$$Y' = k \frac{Y_+ - Y_-}{Y_+ + Y_-},$$

where k is the sensitivity of the BPM at 1500 MHz (18.5 mm as recently measured on the test stand), then the beam position is

$$\begin{pmatrix} X \\ Y \end{pmatrix} = \frac{1}{\sqrt{2}} \begin{pmatrix} 1 & -1 \\ 1 & 1 \end{pmatrix} \left[\begin{pmatrix} X' \\ Y' \end{pmatrix} - \begin{pmatrix} X'_{off} \\ Y'_{off} \end{pmatrix} \right]$$

after rotation by -45° . The offsets X'_{off} and Y'_{off} may be used to save particular (golden) orbits by zeroing the BPM outputs at particular beam defined locations.

How Do the Linac BPMs Work?

Of course there are errors in the system. The first is that the relative amplitude gains in the channels might be different. The second is that offsets exist in the amplitude detector. These sources of error are accounted for by the following modified software computation of the unrotated positions

$$X' = k \frac{(X_+ - X_{off+}) - \alpha_X(X_- - X_{off-})}{(X_+ - X_{off+}) + \alpha_X(X_- - X_{off-})}$$

and

$$Y' = k \frac{(Y_+ - Y_{off+}) - \alpha_Y(Y_- - Y_{off-})}{(Y_+ - Y_{off+}) + \alpha_Y(Y_- - Y_{off-})},$$

where α_X , α_Y , $X_{off\pm}$, and $Y_{off\pm}$ are measured by the so-called automatic calibration circuitry as follows:

- Using the zero wires facility in the software, measure the offset voltages $X_{off\pm}$ and $Y_{off\pm}$ with both the beam and calibration signal off
- Calibrate the X channels with a calibration signal on y_-
- Calibrate the Y channels with a calibration signal on x_-

In both of these final bullets, following diagnostics systems usage, the word "calibrate" means to find the relative gain ratios α_X and α_Y for the X and Y channels respectively. This is done by measuring the amplitude ratio when the calibration signal is on:

$$\alpha_X = \frac{X_+ - X_{off+}}{X_- - X_{off-}} \quad (1)$$

and

$$\alpha_Y = \frac{Y_+ - Y_{off+}}{Y_- - Y_{off-}}. \quad (2)$$

For this calibration to be complete, it is implicit that the *only signal source during the calibration procedure is that from the calibration source*. Unfortunately, this is not the case for the present linac monitors unless all of the RF systems near the monitor to be calibrated are turned off.

Therefore, it should be clear that the diagnostics system definition of the word "calibrate" is different than the usual definition of the word. When a physicist uses the word calibrate the meaning is: Don't tell me the details of how it's done, just tell me that you have a checked procedure that ensures that the displayed results are *real relative positions*. As of now, this has never successfully occurred with the linac monitors when they have been operated at 1500 MHz, and only occasionally been done when they were used at 100 MHz. The problem is RF feedthrough.

If the monitor is "calibrated" as above, and if the only signal processed in the tunnel electronics were that from the beam, then the output positions would be accurately computed and displayed. Because one usually wants to use the BPM when the RF systems are

in fact on, it is not so. The linac BPM electronics pick up signals from RF feedthrough that corresponds to roughly $10 \mu\text{A}$ beam current, a typical current value during beam measurements. Therefore, there is an offset voltage in the amplitude detector which destroys the accuracy of the displayed readings. Trying to calibrate with the RF on is useless because the calibration signal and the feedthrough are the same order of magnitude, but at essentially arbitrary phase, meaning that relative gains as computed using Eqns. (1) and (2) are not correct.

What to Do

There are four basic methods to solve this problem:

- Increase the beam signal compared to the feedthrough noise signal
- Decrease the feedthrough noise signal to acceptable levels
- Add a way to detect the noise phase and correct in software
- Linearize and cross-calibrate with a viewer

None of them is easy. The first method means to replace the existing monitors with a higher sensitivity design. A test of a SLAC design is currently underway in order to determine how much can be gained this way. The second method means either to better shield the sensitive tunnel electronics from fundamental RF noise, or to change the carrier frequency to 500 MHz or 3 GHz, which are frequencies in the beam current away from the fundamental. The third method means adding 1 MHz phase detection circuitry to the revised B0007 that will be used for the linac systems and modifying the software computation. Using the fourth method means that one can do no better than the viewer in accuracy.

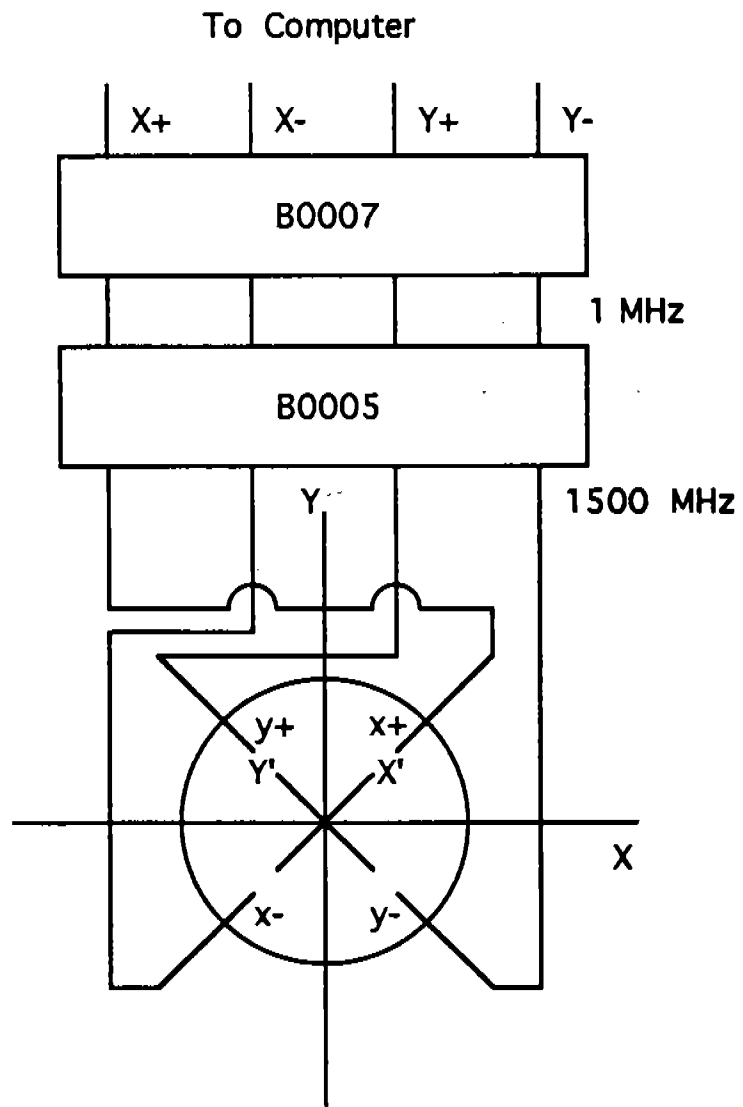


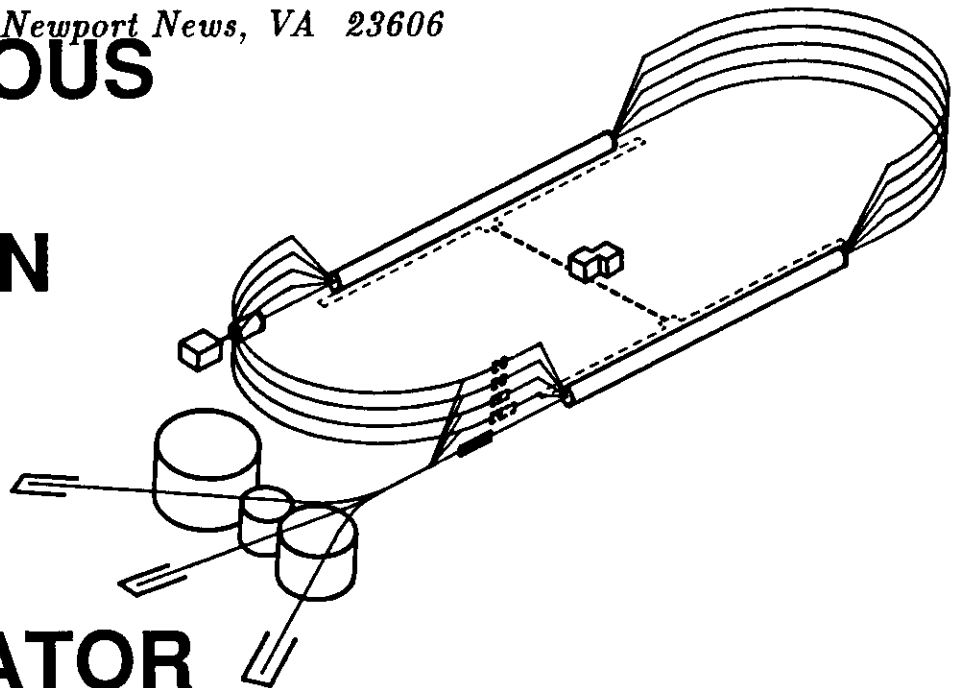
**Fig. 1 Modified Linac Beam Position Monitor
Detection Scheme**

CEBAF PR-90-024
October 1990

**A General Analysis of Thin Wire Pickups
for High Frequency Beam Position Monitors**

*Walter Barry
Continuous Electron Beam Accelerator Facility
12000 Jefferson Avenue
Newport News, VA 23606*

CONTINUOUS
ELECTRON
BEAM
ACCCELERATOR
FACILITY



SURA Southeastern Universities Research Association

CEBAF
The Continuous Electron Beam Accelerator Facility
Newport News, Virginia

Copies available from:

Library
CEBAF
12000 Jefferson Avenue
Newport News
Virginia 23606

The Southeastern Universities Research Association (SURA) operates the Continuous Electron Beam Accelerator Facility for the United States Department of Energy under contract DE-AC05-84ER40150.

DISCLAIMER

This report was prepared as an account of work sponsored by the United States government. Neither the United States nor the United States Department of Energy, nor any of their employees, makes any warranty, express or implied, or assumes any legal liability or responsibility for the accuracy, completeness, or usefulness of any information, apparatus, product, or process disclosed, or represents that its use would not infringe privately owned rights. Reference herein to any specific commercial product, process, or service by trade name, mark, manufacturer, or otherwise, does not necessarily constitute or imply its endorsement, recommendation, or favoring by the United States government or any agency thereof. The views and opinions of authors expressed herein do not necessarily state or reflect those of the United States government or any agency thereof.

A GENERAL ANALYSIS OF THIN WIRE PICKUPS FOR HIGH FREQUENCY BEAM POSITION MONITORS*

W. Barry

Continuous Electron Beam Accelerator Facility
12000 Jefferson Avenue, Newport News, VA 23606

Abstract

In many particle accelerators, a large number of high frequency beam position monitors (BPMs) are required to track and correct the orbit of the beam. Therefore, simple, sensitive, low cost pickup designs for such BPMs are of widespread interest. In this paper, a general analysis of arbitrarily terminated thin wire stripline or "wireline" pickups for BPMs is presented. Subsequently, three specific cases of interest, the open-circuited end, short-circuited end, and matched end wirelines are compared and contrasted in detail. Of these three cases, the open-ended wireline pickup BPM is found to be particularly well-suited for application in the arc regions of the Continuous Electron Beam Accelerator Facility (CEBAF). Measurements of a 1.5 GHz prototype of this type of BPM yielded a longitudinal (sum) pickup impedance of 72Ω , a transverse pickup impedance of $3.8 \Omega/\text{mm}$, and a bandwidth of 470 MHz, all of which are in excellent agreement with the theory.

Introduction

It is presently estimated that 400–600 microwave BPMs operating at the machine frequency (1.497 GHz) are required for the CEBAF accelerator. Because of the large number of monitors involved, a simple low cost pickup design is of primary concern. In addition, the BPMs must be capable of accurately measuring the position of beams with average currents as low as $1 \mu\text{A}$. For the extremely short bunch length at CEBAF, this results in a $2 \mu\text{A}$ AC component of beam current at 1.497 GHz. Consequently, the BPMs must be extremely sensitive as well as inexpensive.

A BPM pickup design well-suited to this application consists of a thin quarter wavelength antenna or "wireline" inside the beampipe and is similar to the standard stripline pickup design. However, in the present design, only the upstream end of the line is terminated, and the line impedance is not necessarily matched to the termination impedance. This results in a non-directional broadband pickup that, apart from a geometric factor, depends solely on the wireline impedance. This latter feature is most important because in practice, the line impedance can be made as high as 200Ω which is a factor of four greater than the standard termination impedance of 50Ω available at microwave frequencies.

The unterminated downstream or open-ended wireline pickup is a specific case of the more general wireline pickup with arbitrary upstream and downstream terminations. In this paper, a general analysis of the ideal wireline pickup is given. The characteristics of the open-ended wireline pickup are then discussed and compared to those of the conventional

* This work was supported by the U.S. Department of Energy under contract DE-AC05-84ER40150.

matched stripline and shorted-end or “loop” pickups which are presently in use in the CEBAF linacs.^[1] In addition, the results of longitudinal and transverse bench tests on an open-ended pickup BPM which confirm the theory are presented.

Response Functions for Wireline Pickups

The BPM to be considered is illustrated schematically in figure 1. The monitor consists of four thin wire antennas (x plane shown in figure 1) located orthogonally to each other inside a circular beampipe of radius a . Each wire has length ℓ , diameter d and is located a distance b from the centerline of the monitor. As with conventional stripline pickups, each wire forms a transmission line with characteristic impedance Z_c determined by the dimensions a , b , and d . For the general wireline pickup, the output is terminated by a load impedance Z_1 , and the downstream end is terminated with an impedance Z_2 .

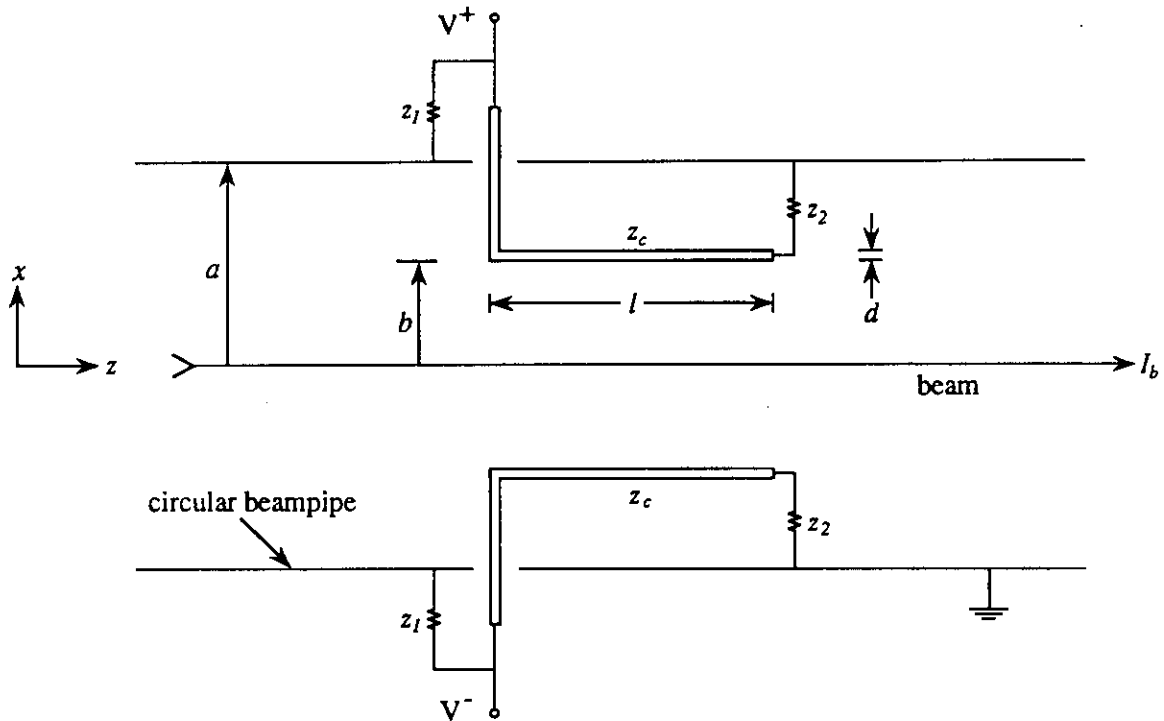


Figure 1 General wireline pickup BPM.

The goal of the analysis is to derive the frequency and impulse responses of the wireline pickup for arbitrary real impedances Z_1 , Z_2 , and Z_c . Subsequently, the special cases of the conventional stripline ($Z_1 = Z_2 = Z_c$), open-ended wireline ($Z_2 = \infty$) and shorted-end wireline or “loop pickup” ($Z_2 = 0$) can be examined in greater detail. In addition, the longitudinal and transverse pickup impedances for the open-ended monitor are derived.

It is well established through the application of the Lorentz reciprocity and Panofsky-Wenzel theorems that beam currents couple to pickups only in regions where electric fields parallel to the current exist when the pickup is driven as a kicker.^[2] For the pickups in

figure 1, these regions must be the discontinuities at the upstream and downstream ends of the wirelines because, when driven as kickers, the wirelines support pure TEM modes except at these locations. Assuming the longitudinal electric kicker fields are localized at these locations, a reasonable equivalent circuit, shown in figure 2, for modeling the wireline as a pickup can be devised.

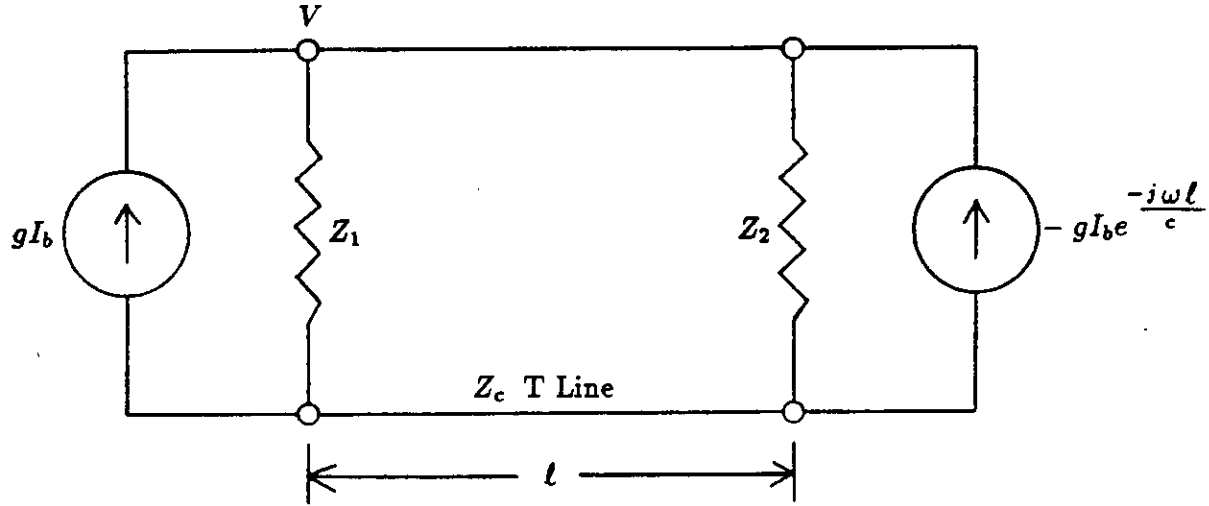


Figure 2 Equivalent circuit for general wireline pickup.

The equivalent circuit, shown in phasor form, consists of the wire transmission line and its associated terminations driven by current sources at the upstream and downstream ends. The magnitude of the sources is the magnitude of the phasor component of beam current, I_b , reduced by a geometric coupling factor, g , which depends on transverse beam position. The downstream source is delayed in phase by $\omega l/c$ to account for the propagation time of the beam. Here, the beam velocity is assumed to be c ($\beta = 1$) for simplicity. In addition, an overall minus sign on the downstream source accounts for the polarity difference between the upstream and downstream ends of the wireline. This polarity difference results because the direction of the beam current relative to the wireline is such that it is “entering” the upstream end of the pickup and “exiting” the downstream end. Equivalently, the downstream source in figure 2 could be drawn in the opposite direction while dropping the minus sign.

The basic quantity of interest is the transfer impedance, Z_T , defined for a single pickup as the output voltage from the pickup divided by I_b for a centered beam. The transfer impedance is generally a complex function of frequency and can be found by analyzing the equivalent circuit in figure 2. By applying the principle of superposition to the current sources and using standard transmission line analysis, the transfer impedance for the equivalent circuit model is found to be:

$$Z_T(\omega) = \frac{gZ_1 \parallel Z_c \left(1 - e^{-j\frac{2\omega l}{c}}\right)}{1 - \Gamma_1 \Gamma_2 e^{-j\frac{2\omega l}{c}}} \quad \Omega \quad (1)$$

where:

$$Z_1 || Z_c = \frac{Z_1 Z_c}{Z_1 + Z_c}$$

$$\Gamma_1 = \frac{Z_1 - Z_c}{Z_1 + Z_c}$$

$$\Gamma_2 = \frac{Z_2 - Z_c}{Z_2 + Z_c}$$

For real frequency independent terminations Z_1 and Z_2 , the corresponding reflection coefficients Γ_1 and Γ_2 are also real and independent of frequency. In this case, the unit impulse response of the wireline pickup is readily obtained from the inverse Laplace transform of equation (1). The resulting impulse response is given as:

$$z_T(t) = g Z_1 || Z_c \left\{ \delta(t) + \left(1 - \frac{1}{\Gamma_1 \Gamma_2} \right) \sum_{n=1}^{\infty} (\Gamma_1 \Gamma_2)^n \delta \left(t - \frac{2n\ell}{c} \right) \right\} \quad \Omega/\text{sec} \quad (2)$$

Having the unit impulse response, the voltage at the output of the pickup for a beam current with arbitrary time dependence $i_b(t)$ may be found by convolution:

$$v(t) = \int_0^{\infty} i_b(\tau) z_T(t - \tau) d\tau \quad (3)$$

Expressions (1) and (2) completely characterize the general wireline pickup. However, at this point, three important specific cases of the wireline pickup are examined in more detail. The three pickup types of interest include the matched wireline ($Z_1 = Z_2 = Z_c$), the open-circuited wireline ($Z_2 = \infty$), and the short-circuited wireline ($Z_2 = 0$). In all cases, the transfer impedance given by equation (1) is a maximum at the frequency where ℓ is a quarter wavelength long. Designating this frequency ω_0 and using the relation $\pi/\omega_0 = 2\ell/c = t_0$, expressions for the amplitude and phase of the transfer impedance for the three pickup types, shown in table 1, may be derived from equation (1). In addition, table 1 contains expressions for the 3 dB bandwidth and unit impulse response for each pickup type.

Several observations about the three pickup types can be made from table 1. All three pickups exhibit repeated symmetric band pass characteristics centered at odd integer multiples of ω_0 . Although theoretically these pass bands repeat indefinitely with increasing frequency, several effects not incorporated into the theory presented here limit the high frequency response of the pickups. As the frequency increases beyond cutoff for the lowest order TM waveguide mode in the beampipe ($f_c = .383 c/a$), an increasing number of waveguide modes can be excited, significantly altering the response of the pickup. At extremely high frequencies, the possibility of higher order modes on the wirelines themselves exists. In view of these and other high frequency effects, the practical operating range of the pickups is usually limited to the fundamental bandpass region centered at ω_0 .

**Table 1. Frequency and Impulse Characteristics
of Various Wireline Pickups**

	Matched Line	Open Circuit Line	Short Circuit Line
$ Z_T $	$gZ_1 \sin \theta $	$\frac{gZ_c \sin \theta }{\sqrt{R^2 \cos^2 \theta + \sin^2 \theta}}$	$\frac{gZ_1 \sin \theta }{\sqrt{R^{-2} \cos^2 \theta + \sin^2 \theta}}$
$\angle Z_T$	$\frac{\pi}{2} - \theta$	$\tan^{-1}(R \cot \theta)$	$\tan^{-1}(R^{-1} \cot \theta)$
$\Delta\omega_{3dB}$	ω_0	$2\omega_0 \left(1 - \frac{2}{\pi} \tan^{-1} R\right)$	$2\omega_0 \left(1 - \frac{2}{\pi} \tan^{-1} R^{-1}\right)$
$z_T(t)$	$g\frac{Z_1}{2} [\delta(t) - \delta(t - t_0)]$	$gZ_1 \ Z_c \left\{ \delta(t) + \left(1 - \frac{1}{\pm\Gamma_1}\right) \sum_{n=1}^{\infty} (\pm\Gamma_1)^n \delta(t - nt_0) \right\}$	

Notes: $R = Z_c/Z_1$ + for open line
 $\theta = \frac{\pi}{2} \frac{\omega}{\omega_0}$ - for shorted line
 $t_0 = 2\ell/c$

As can be seen from table 1, the 3 dB bandwidths of the bandpass regions for all three pickups depend on the ratio of line impedance to load impedance (R). As this ratio is increased from zero to infinity, the bandwidth of the open circuit pickup decreases from $2\omega_0$ to zero, whereas the bandwidth of the short circuit pickup increases from zero to $2\omega_0$. For $R = 1$ (matched line case) the bandwidth is ω_0 , and in addition the transfer impedances of the open- and short-circuited pickups reduce to that of the matched line pickup. This is consistent with the well-known property of pickup response being independent of the downstream termination for conventional stripline pickups. It should be pointed out that, although the pickup responses of the open and short circuit pickups reduce to that of the matched line for $R = 1$, these pickups are always non-directional regardless of the value of R , whereas the true matched line pickup is completely directional. These directionality properties (not embodied in table 1) can be verified by considering an equivalent circuit similar to that of figure 2 for a beam travelling in the opposite direction. Performing this calculation reveals that all pickups with $Z_1 = Z_2$ are always completely directional, the open and short circuit line pickups ($Z_2 = \infty$, $Z_2 = 0$) are always non-directional, and all other cases exhibit partial directionality.

Perhaps the most important characteristic of the three pickups is $|Z_T|$ at center frequency ($\omega = \omega_0$). From table 1, $|Z_T(\omega_0)|$ is seen to be strictly proportional to the load impedance, Z_1 , for the matched and short-circuited line pickups. In the case of the open-circuited line pickup, $|Z_T(\omega_0)|$ is proportional to the line impedance, Z_c , and is independent of the loading. These properties illustrate the duality between the open-circuited line pickup and short-circuited line pickup for at ω_0 , the former can be modeled as an ideal voltage source of strength $gZ_c I_b$ and the latter as an ideal current source of strength gI_b .

Typically, the characteristic impedance of a wireline pickup can be made as high as 200 Ω , which is a factor of four greater than the standard termination impedance of 50 Ω available at microwave frequencies. Therefore, at microwave frequencies, a BPM utilizing open-circuited wireline pickups offers up to four times the sensitivity of the traditional

matched line pickup BPM. Of course, as with all pickups, this increase in sensitivity brings with it a decrease in bandwidth. From the open-circuited line bandwidth equation in table 1, a calculation of 3 dB bandwidth for $R = 200 \Omega / 50 \Omega = 4$ gives approximately $\omega_0/3$ or $Q \approx 3$. However, this is still a relatively broadband device, and in applications where beam position measurements are made using a single CW harmonic of the accelerator RF (as in the CEBAF arcs), extremely large bandwidth is generally of little concern any way.

To further emphasize the properties described above, plots of the amplitude and phase of the transfer impedance for the three pickup types are shown in figures 3 and 4. The amplitude plots are normalized to gZ_1 and carried out to $4\omega_0$ to emphasize the relative sensitivities and multiple bandpass characteristics of the pickups. The amplitude plots confirm all of the characteristics described above. The phase plots are self-evident with the following major features: the matched line phase is linear with frequency, the open-circuited line phase takes on a resonant circuit characteristic, and the short-circuited line phase has an inverted resonant shape with a constant phase band about ω_0 .

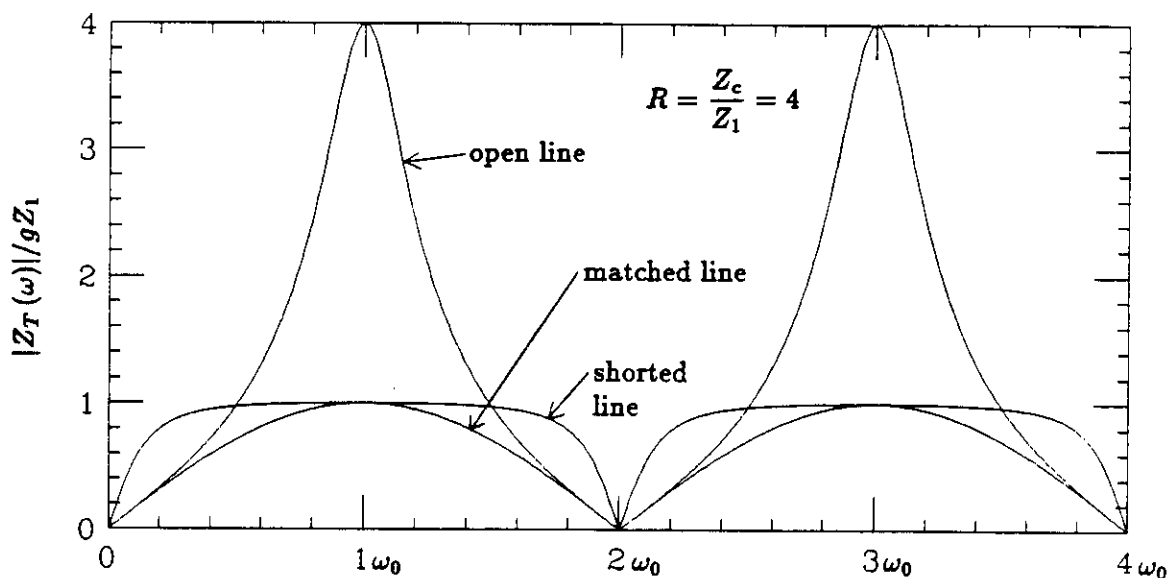


Figure 3 Amplitude of transfer impedance vs. frequency.

It is also noted from the amplitude plots that the low frequency response of the short-circuited line pickup is considerably better than that of the matched line or open-circuited line pickup. This suggests the use of short-circuited line or "inductive loop" pickups in low frequency applications where quarter wavelength pickups are impractical. These loop pickups are currently being utilized in the CEBAF linac BPMs where a 100 MHz beam current modulation is detected.^[1] In general, it can be concluded that in virtually every application in which a conventional matched line BPM can be used, an open- or short-circuited line BPM can be used with a possible increase in performance and with a reduced cost because complicated downstream terminations are eliminated. Notable exceptions to this include applications where directionality is required or where the pickups are also used

as kickers. It is pointed out that when used as kickers, the open and short-circuited lines present reactive loads and are therefore incompatible with most high power/high frequency sources.

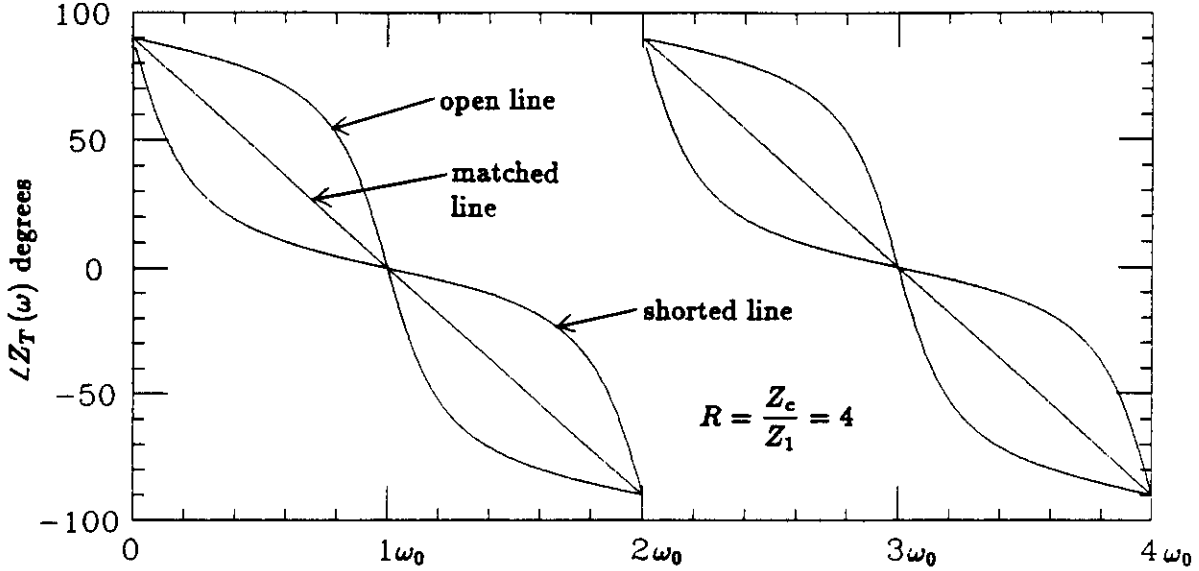


Figure 4 Phase of transfer impedance vs. frequency.

For completeness, the impulse responses of the three pickup types with $Z_1 = 50 \Omega$ and $Z_c = 200 \Omega$ are presented in figure 5. The impulse response of the matched line consists of the well-known pair of impulses of height $Z_1 \parallel Z_c = 25 \Omega$ and separated by twice the transit time of the pickup, $t_0 = 2\ell/c$. In the case of the open-circuited pickup, the first pulse has height $Z_1 \parallel Z_c = 40 \Omega$. The second pulse has height $1 + \Gamma_1$ times the sum of the induced downstream pulse, $-Z_2 \parallel Z_c = -Z_c$, and the reflected first pulse. The amplitude of the pulses at the output terminal then decrease geometrically with $\Gamma_1 \Gamma_2 = \Gamma_1$ as the second pulse reflects back and forth along the line. Because Γ_1 is negative, the output pulses alternate in sign. Finally, in the case of the shorted-line pickup, the first pulse amplitude is again $Z_1 \parallel Z_c$. However, because $Z_2 = 0$, no voltage can be induced at the downstream end of the pickup and $\Gamma_2 = -1$. Therefore, the second output pulse has amplitude $-(1 + \Gamma_1)$ times that of the first pulse. The output pulses then decrease geometrically with $-\Gamma_1$. This time, since Γ_1 is negative, the pulses are all of the same sign (that of the second pulse).

As stated in the introduction, a very large number of microwave BPMs are required for the arc regions of the CEBAF accelerator. These BPMs are required to respond to CW beam currents as low as $2 \mu A$ and below at the fundamental RF frequency of 1.497 GHz. In view of the pickup properties described above, it is obvious that the quarter wave open-circuited wireline BPM is technically best suited for this application. In addition, this type of BPM is desirable from a practical standpoint because the simple wire pickups and absence of downstream terminations make it inexpensive and easy to construct. The remainder of this paper describes in more detail the characteristics of the open-circuited pickup BPM, along with results from bench tests of a prototype.

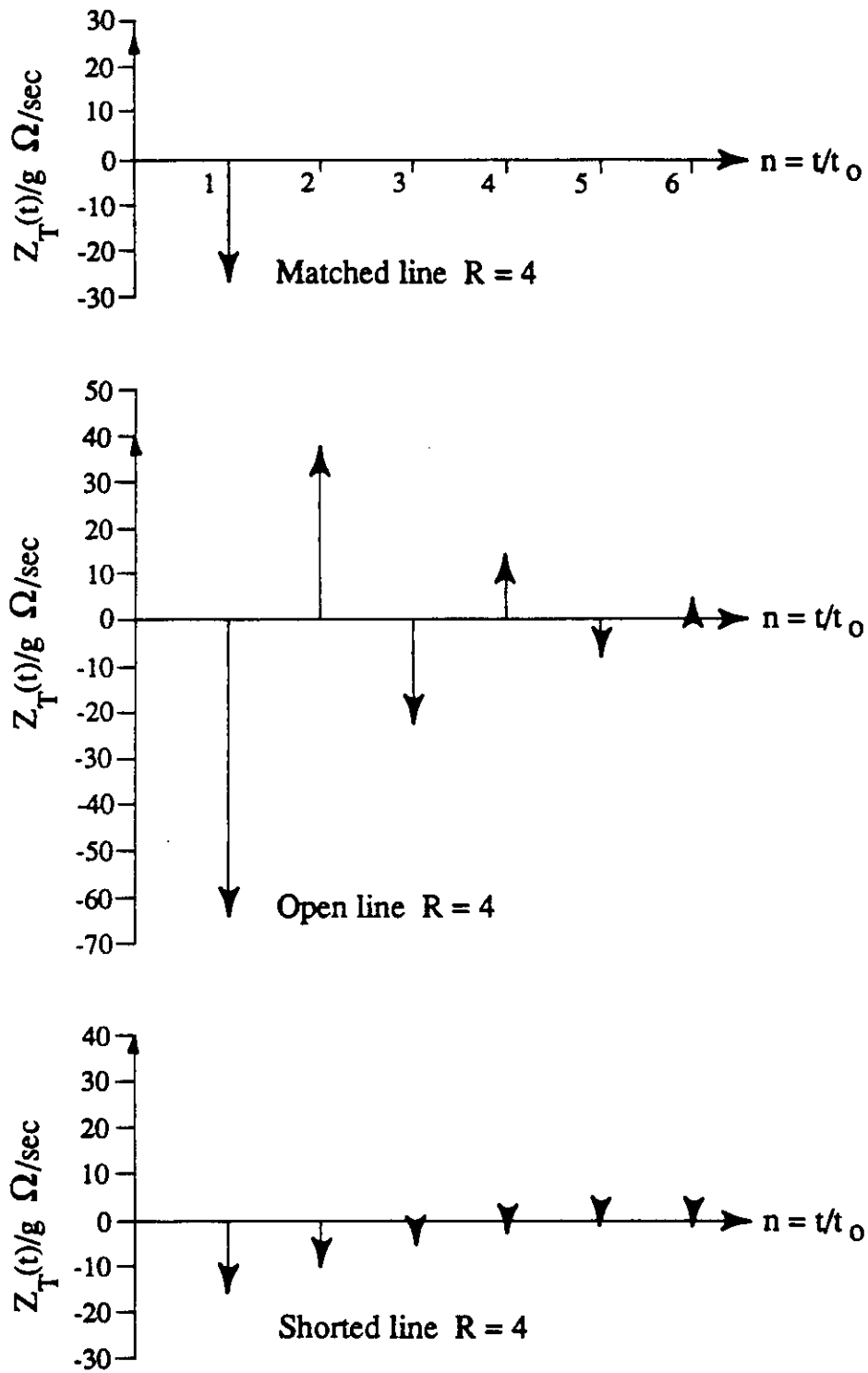


Figure 5 Impulse response of wireline pickups.

Longitudinal and Transverse Impedances of Open-Ended Wireline Pickups

In order to absolutely characterize the open-ended or any wireline pickup, the geometric coupling factor, g , must be determined. The coupling factor depends only on the wireline geometry and hence is independent of frequency and line terminations. Therefore, to calculate g , consider the transfer impedance given by equation (1) for the short-circuited wireline case at very low frequencies:

$$Z_T(\omega) \approx \frac{jg\omega LZ_1}{Z_1 + j\omega L} \quad \Omega \quad Z_2 = 0, \quad \frac{\ell}{\lambda} \ll 1 \quad (4)$$

where:

$$L = \frac{Z_c \ell}{c} \quad \text{henries}$$

In equation (4), L is the total self-inductance of the "loop" formed by the short-circuited wireline. At low frequencies, the total voltage coupled to the loop is proportional to the time rate of change of magnetic flux from the beam passing normally through the loop. This coupling is conveniently quantified by the mutual inductance, M , between the beam current and the pickup loop. This leads to a simple lumped element equivalent circuit for the short-circuited line pickup at low frequencies (figure 6). A trivial analysis of this circuit gives the following result for the transfer impedance:

$$Z_T(\omega) = \frac{V}{I_b} = \frac{j\omega M_0 Z_1}{Z_1 + j\omega L} \quad \Omega \quad (5)$$

where: M_0 = mutual inductance between a centered beam and the loop pickup

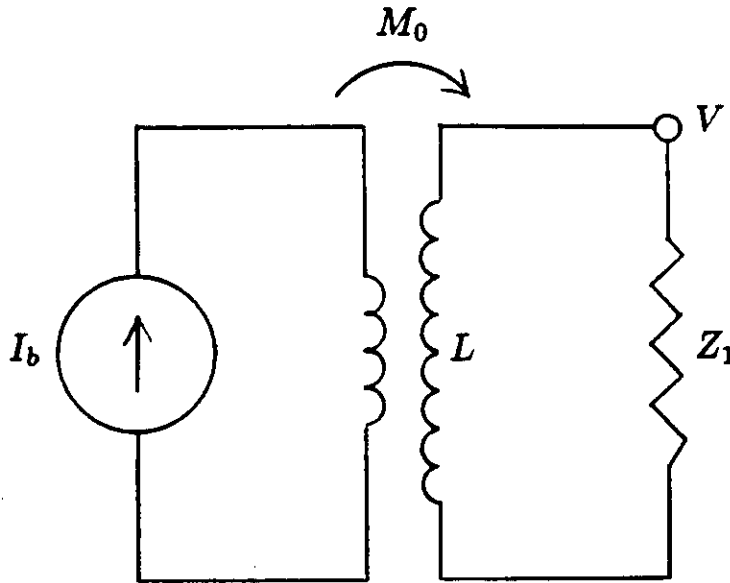


Figure 6 Low frequency equivalent circuit for short-circuited line pickup.

Comparing this expression to (4) gives $g = M_0/L$ or equivalently M'_0/L' where the primes indicate per unit length. The conclusion is that the g factor for all thin wireline type pickups is given by the ratio of mutual inductance per unit length between the beam and the pickup to the self-inductance per unit length of the pickup.

In general, the mutual inductance per unit length between the beam current and a wireline depends on the position of the beam. Referring to the geometry of figure 1, a solution to Laplaces equation in cylindrical coordinates for magnetic vector potential enables the mutual inductances between the beam and the pickups to be calculated as a function of beam position:

$$M'(r, \theta, \theta_0) = -\frac{\mu_0}{2\pi} \left\{ \ln \frac{b}{a} + \sum_{n=1}^{\infty} \frac{1}{n} \left(\frac{r}{a} \right)^n \left[\left(\frac{b}{a} \right)^n - \left(\frac{a}{b} \right)^n \right] \cos n(\theta - \theta_0) \right\} \quad (6)$$

where: r, θ are transverse beam coordinates
 θ_0 is azimuthal location of pickup
 a, b are as in figure 1

For the $+x$ and $-x$ pickups ($\theta_0 = 0, \pi$) shown in figure 1, equation (6) becomes:

$$M'_{\pm}(r, \theta) = -\frac{\mu_0}{2\pi} \left\{ \ln \frac{b}{a} \pm \sum_{n=1}^{\infty} \frac{1}{n} \left(\frac{r}{a} \right)^n \left[\left(\frac{b}{a} \right)^n - \left(\frac{a}{b} \right)^n \right] \cos n\theta \right\} \quad (7)$$

An expression identical to (7) with $\sin n\theta$ replacing $\cos n\theta$ is obtained for a y-axis pair of pickups. From expressions (6) or (7) for $r = 0$ (centered beam) the following equation for M'_0 is obtained:

$$M'_0 = \frac{\mu_0}{2\pi} \ln \frac{a}{b} \quad \text{henries/m} \quad (8)$$

Upon substituting (8) into the definition of g and using the relation $L' = Z_c/c$, a simple expression for the open-circuited wireline pickup transfer impedance at center frequency is obtained from $Z_T(\omega_0) = gZ_c$:

$$Z_T(\omega_0) = \frac{\eta}{2\pi} \ln \frac{a}{b} \quad \Omega \quad (9)$$

where: $\eta = \mu_0 c = 377 \Omega$

Two important quantities for describing the performance of a BPM are the longitudinal and transverse pickup impedances. Referring to the pickup pair in figure 1, these impedances are defined for $\omega = \omega_0$ as follows:

$$Z_{\parallel} = \frac{V^+ + V^-}{I_b} \quad \Omega \quad (10)$$

$$Z_{\perp} = \frac{\partial(V^+ - V^-)}{I_b \partial x} \approx \frac{V^+ - V^-}{I_b x} \quad \Omega/\text{m} \quad (11)$$

where: x = transverse beam position

Using equations (10), (7) and the equivalent circuit of figure 2, the longitudinal pickup impedance of the open-circuited wireline pair becomes:

$$Z_{\parallel} = \frac{M'_+ + M'_-}{L'} Z_c = \frac{\eta}{\pi} \ln \frac{a}{b} \quad \Omega \quad (12)$$

From equation (9), Z_{\parallel} is seen to be equal to $2Z_T(\omega_0)$. The most important feature of Z_{\parallel} for wireline BPMs is that it is independent of beam position. In fact, it is easily verified using equation (6) that the sum of the voltages from any pair of diametrically opposed wireline pickups is completely independent of beam position. This is generally not true for pickup geometries other than that of the wireline. Because the sum voltage is position independent, the wireline BPM is also quite useful in applications requiring position independent measurements of beam current amplitude and phase. Examples of these kinds of measurements at CEBAF include absolute beam current and a proposed bunch length measurement technique.^[3]

The transverse pickup impedance is most easily obtained by relating it to Z_{\parallel} . From definitions (10) and (11):

$$Z_{\perp} = Z_{\parallel} \frac{\partial(\Delta/\Sigma)}{\partial x} \quad \Omega/\text{m} \quad (13)$$

where:

$$\Delta/\Sigma = \frac{V^+ - V^-}{V^+ + V^-}$$

The difference over sum voltage, Δ/Σ , is linearly related to beam position throughout 40% or more of the aperture defined by the pickups and is the standard quantity used to determine beam position in most BPM systems. For a pair of identical wireline pickups, the difference over sum voltage ratio is also equal to $(M'_+ - M'_-)/(M'_+ + M'_-)$. Using equation (7) to first order, a simple but accurate approximation for the slope of the difference to sum voltage vs. position curve is obtained:

$$\frac{\partial(\Delta/\Sigma)}{\partial x} = \frac{(\frac{a}{b} - \frac{b}{a})}{a \ln \frac{a}{b}} \approx \frac{2}{a} \quad \text{m}^{-1} \quad (14)$$

Therefore for the open-circuited wireline BPM:

$$Z_{\perp} \approx \frac{2}{a} Z_{\parallel} = \frac{2\eta}{\pi a} \ln \frac{a}{b} \quad \Omega/\text{m} \quad (15)$$

Equations (9), (12), (14), and (15) characterize the absolute longitudinal and transverse sensitivity of the open-circuited wireline BPM. The transfer, longitudinal and transverse pickup impedances of the matched and short-circuited line BPMs may be obtained by dividing equations (9), (12), and (15) by the ratio $R = Z_c/Z_1$.

Bench Tests of Prototype BPM

A mechanical drawing of a 1.497 GHz prototype open-circuited wireline BPM for use in the CEBAF arc regions is shown in figure 7. The monitor consists of a 2.75" beam tube with four simple wire antennas connected to Ceramaseal ultra-high vacuum SMA feedthroughs. The wire lengths have been trimmed for peak response at 1.497 GHz. Using the dimensions given on the drawing, the theoretical impedance values for the monitor can be computed using equations (9), (12), and (15) giving: $Z_T(\omega_0) = 36.1 \Omega$, $Z_{\parallel} = 72.2 \Omega$, and $Z_{\perp} = 4.3 \Omega/\text{mm}$. In addition, the ratio factor, $R = Z_c/Z_1$, can be computed using the following formula for the characteristic impedance of an eccentric wire transmission line:^[4]

$$Z_c = \frac{\eta}{2\pi} \cosh^{-1} \left\{ \frac{a}{d} \left[1 - \left(\frac{b}{a} \right)^2 \right] + \frac{d}{4a} \right\} \quad (16)$$

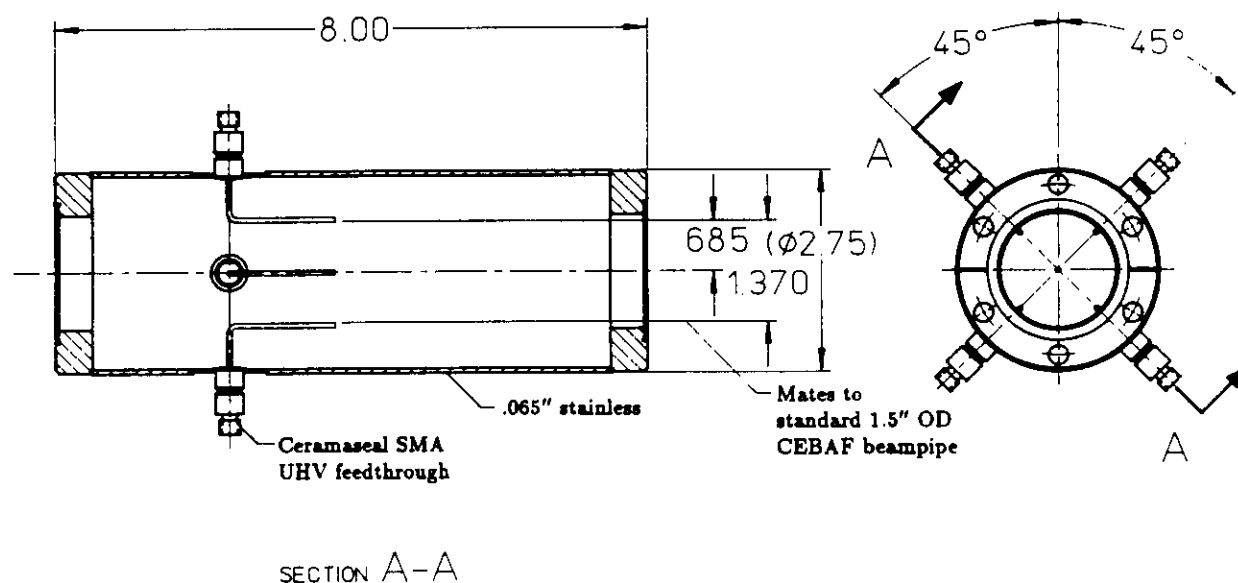


Figure 7 Open-circuited wireline BPM.

Using the pickup dimensions given in figure 7, $Z_c = 200 \Omega$, and $R = 4$ for $Z_1 = 50 \Omega$. Therefore, $Z_T(\omega)$ for the prototype should be given by the open-circuited line curves of figures 4 and 5 with $|Z_T| = 36.1 \Omega$ at $\omega_0 = 2\pi \times 1.497 \text{ GHz}$.

To measure the impedances of the prototype, the standard technique employing a thin current carrying wire stretched through the center of the monitor to simulate the beam was used. The transfer impedance as a function of frequency is then obtained by measuring S_{21} with a microwave network analyzer. As indicated in figure 8, the stretched wire inside the BPM forms a transmission line with characteristic impedance Z_L . In order to ensure that only a forward current wave exists on the wire, the line must be matched at the downstream end. In addition, matching to the 50Ω system of the network analyzer at the upstream end ensures all of the incident power is transmitted into the monitor. As shown,

the upstream and downstream matching from Z_ℓ to 50Ω is obtained with broadband multiple quarter wavelength section transformers. Knowing that all of the incident power is transmitted to the line inside the monitor, it is simple to relate $Z_T(\omega) = V^-/I_\ell$ to $S_{21}(\omega) = V^-/V^+$:

$$Z_T(\omega) = S_{21}(\omega)\sqrt{50 Z_\ell} \quad \Omega \quad (17)$$

For the test configuration used, the stretched wire diameter was .118" (3 mm) so that $Z_\ell = 186 \Omega$. Therefore, from equation (17), $Z_T = 96.4 S_{21}$.

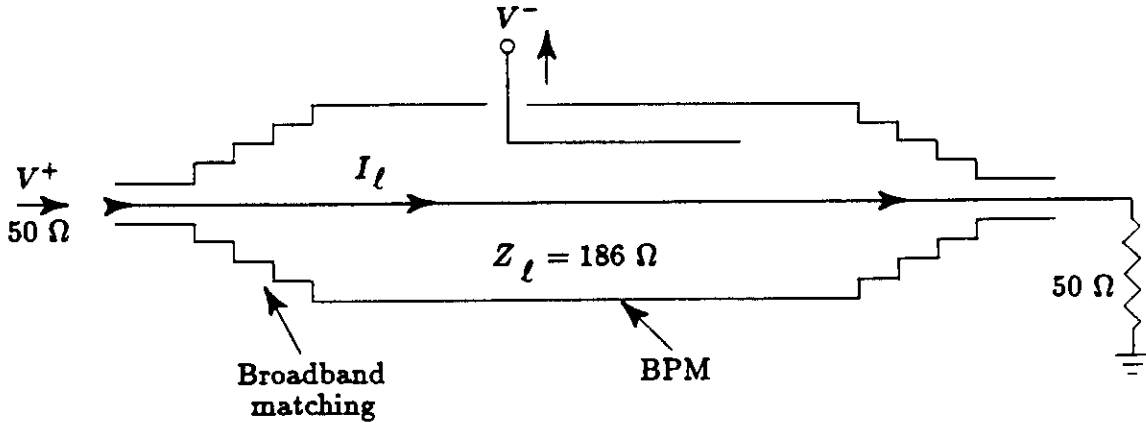


Figure 8 Wire technique for measuring BPM impedance.

Plots of S_{21} amplitude and phase measured for a single pickup of the prototype monitor over the frequency range .5 to 2.5 GHz are given in figure 9. At center frequency, $|Z_T(\omega_0)|$ is $96.4 \times .375 = 36.1 \Omega$, which is in exact agreement with the theoretical impedance. Also contained in figure 9 are plots of the theoretical amplitude and phase (dashed) of $S_{21}(\omega)$ obtained from the equations in table 1 for $R = 4$ and equation (17). Both amplitude and phase show good agreement with the measured data over the entire 2 GHz band. It is pointed out here that the SMA vacuum feedthroughs used on the prototype were the non-50 Ω type which obviously work quite well. This is quite fortunate because the 50 Ω versions cost five to six times as much as the non-50 Ω feedthroughs.

The transverse properties of the prototype were measured by moving the stretched wire in the transverse plane of the monitor along the line adjoining a pair of pickups. For each wire position the difference over sum voltage ratio for the plus and minus pickup pair was measured in terms of S_{21} :

$$\frac{\Delta}{\Sigma} = \frac{S_{21}^+ - S_{21}^-}{S_{21}^+ + S_{21}^-} \quad (18)$$

The position of the wire relative to the monitor was changed by fixing the wire and matching sections and moving the monitor with a precision micro-adjustable stage. Of course, once the wire is moved off center it is no longer matched to 50 Ω , especially for extreme transverse positions. However, because the quantity of interest is the ratio of difference over sum S_{21} , the reflections caused by the mismatches are of no concern.

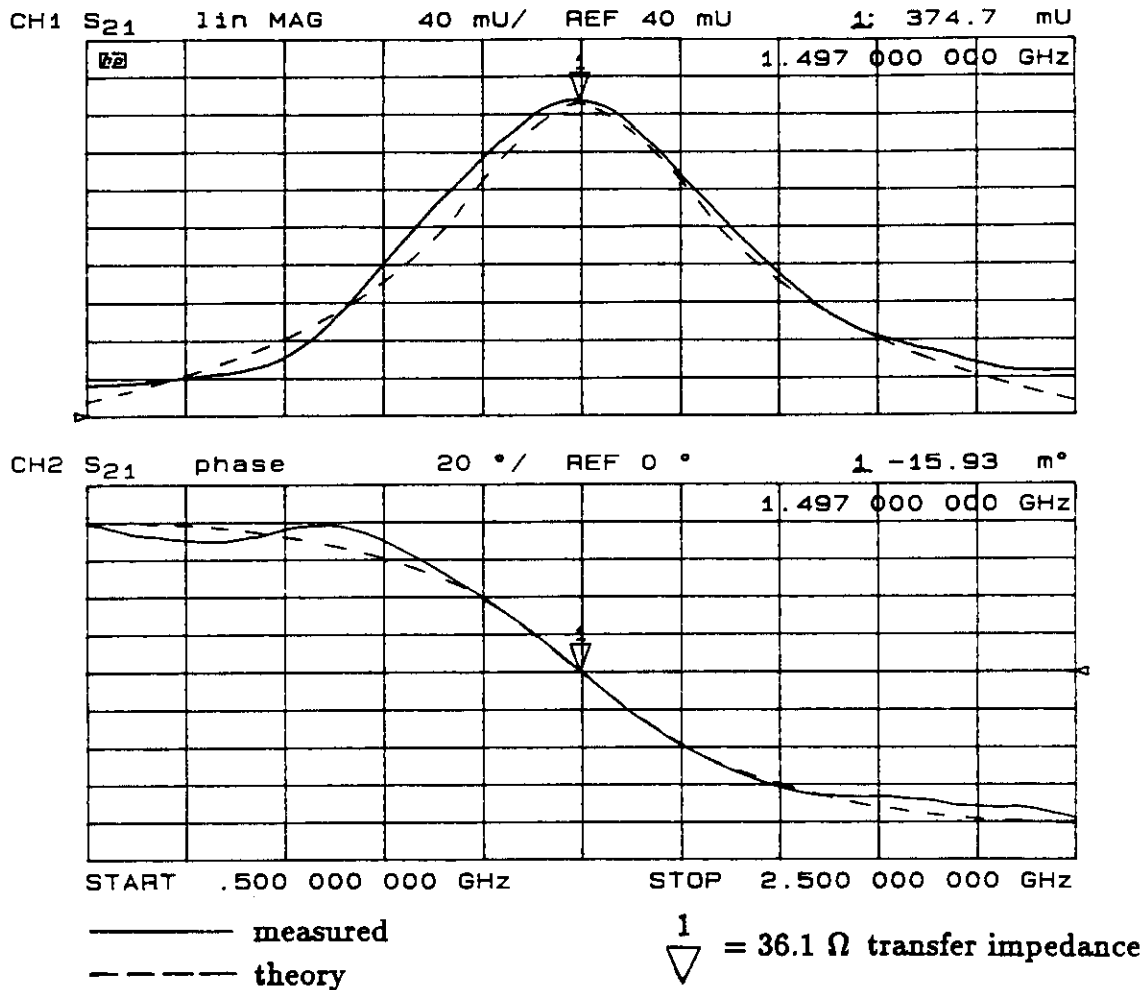


Figure 9 S₂₁ amplitude and phase for open-circuited wireline BPM prototype.

Figure 10 shows a plot of difference over sum voltage vs. transverse wire position for a pickup pair in the prototype BPM. As shown, Δ/Σ is linear with position over a ± 8 mm range and has slope $\partial(\Delta/\Sigma)/\partial x = .053 \text{ mm}^{-1}$, which is within 12% of the approximate theoretical value given by $2/a = .060 \text{ mm}^{-1}$. This small difference between theory and measurement is attributed to the idealized calculation of transverse pickup response which does not include the effect of the radial section of wire connecting the feedthrough to the section of the pickup parallel to the beam. Therefore, the accuracy of the theory should increase as the ratio b/a gets larger. This is in fact found to be the case. Transverse measurements on another model BPM with b/a 10% greater than the prototype described here yielded 6% agreement between theory and measurement.

Having measured $\partial(\Delta/\Sigma)/\partial x$, the BPM is completely characterized. In summary, $Z_T(\omega_0) = 36.1 \Omega$, $Z_{\parallel} = 72.2 \Omega$, and $Z_{\perp} = 3.8 \Omega/\text{mm}$ (from equation (13)).

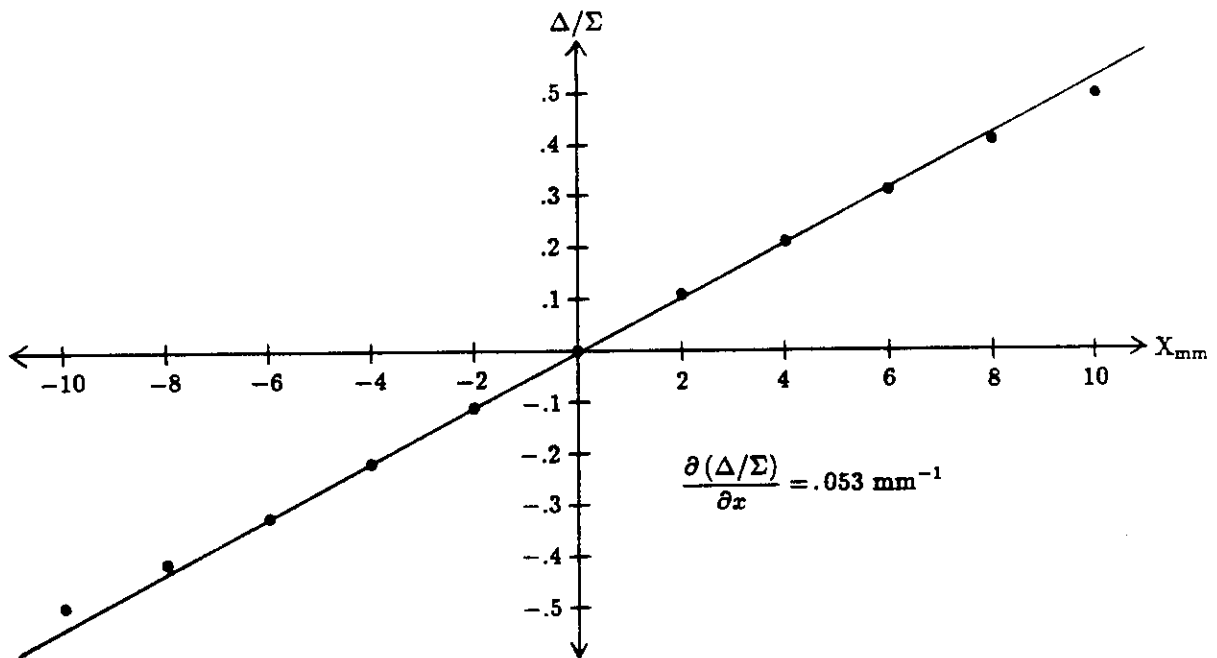


Figure 10 Δ/Σ vs. position measurements for 1.497 GHz BPM.

Summary and Conclusion

A simple and general analysis of wireline pickup BPMs has been presented. Special attention has been paid to three important pickup types: the matched wireline, the open-circuited wireline, and the short-circuited wireline. In particular, the open-circuited wireline is well-suited for application in BPMs for the CEBAF arc regions where 1.497 GHz CW beam currents are detected. The most important characteristics of the open-circuited wireline BPM are: high sensitivity, easy and inexpensive construction, and sum signals that are independent of beam position.

Acknowledgements

The author wishes to thank Karel Capek of CEBAF for the excellent fabrication of BPM prototypes and wire matching sections.

References

- [1] W. Barry, "Inductive Megahertz Beam Position Monitors for CEBAF", CEBAF PR-89-003.
- [2] G. R. Lambertson, "Physics of Particle Accelerators", eds. M. Month and M. Dieres, AIP 153, vol. 1 (1987).
- [3] C. G. Yao, "A Scheme for Measuring Length of Very Short Bunch at CEBAF", Proceedings of the 1990 Workshop on Accelerator Instrumentation, (to be published).
- [4] T. Moreno, Microwave Transmission Data, Artech House, Norwood, MA (1989).

THE TIMING SYNCHRONIZATION SYSTEM AT JEFFERSON LAB*

M. Keesee, R. Dickson, R. Flood, Jefferson Lab,
12000 Jefferson Ave, Newport News, VA 23606, USA
V. Lebedev, Fermi National Accelerator Laboratory
P.O. Box 500, Batavia, IL 60510

Abstract

This paper presents the requirements and design of a Timing Synchronization System (TSS) for the Continuous Electron Beam Accelerator Facility (CEBAF) control system at Thomas Jefferson National Accelerator Facility. We have designed a clock module, which resides in a VME crate. The clock module can be a communications master or a slave depending on its configuration, which is software and jumper selectable. As a master, the clock module sends out messages in response to an external synchronization signal over a serial fiber optic line. As a slave, it receives the messages and interrupts an associated computer in its VME crate. The application that motivated the development of the TSS, the Accelerator 30 Hz Measurement System, will be described. Our operational experience with the TSS will also be discussed.

1 INTRODUCTION

The CEBAF accelerator is a five pass CW recirculator, which can reach an energy of 6.067 GeV. It consists of a 67 MeV injector, two superconducting 600 MeV linacs, and 9 arcs of magnets which connect the linacs for beam recirculation. See figure 1.

In order to improve machine reproducibility and reduce beam tune time, we have developed a '30 Hz measurement system'. By means of a small set of correctors or RF cavities, one can induce a beam perturbation at a frequency of 30 Hz. The effect of this perturbation is apparent at any Beam Position Monitor (BPM) point in the machine.

We enhanced the BPM software to detect beam differential displacements resulting from such a 30 Hz perturbation of lateral beam position or energy. For beam tuning, we use AC line synchronized 60 Hz pulsed beam. The BPM system performs data acquisition at 60 Hz synchronized with this pulse. The choice of 30 Hz as the perturbation frequency enables us to synchronize every other beam pulse to the positive or negative crest of the perturbation signal. It thus becomes important for the BPM systems to be

able to differentiate positive or negative crested data, i.e. the BPMs must maintain synchronization with the 30 Hz perturbation polarity.

Prior to the development of the hardware-based TSS, the implementation of the 30 Hz measurements used a software based synchronization system. This was an accelerator control system network broadcast to inform the BPMs of the polarity of the 30 Hz signal. This approach resulted in a system sensitivity to network delays that occasionally caused the BPM system to label the data with the wrong polarity. It therefore became apparent that a different approach was needed.

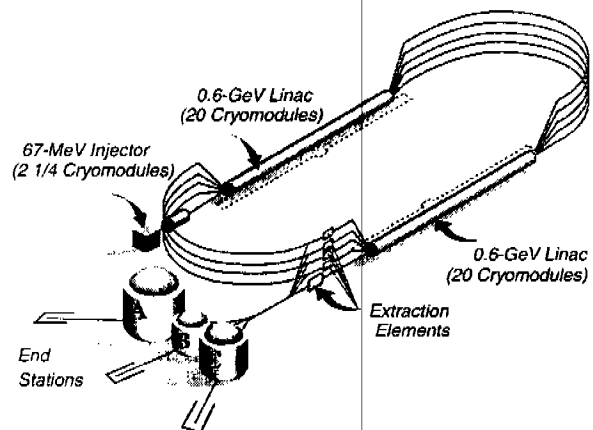


Figure 1. Machine Configuration

2 SYSTEM OVERVIEW

The hardware-based TSS uses one master clock module and multiple slave clock modules [1]. These 3U sized cards share the VME bus with the control system's front end Input-Output Controllers (IOCs). There are IOCs at many locations around the accelerator. The communication flow, from master to slave boards, occurs over a single fiber optic line originating from the master. Each card has a fiber optic receiver and repeating transmitter. The last card in the chain is connected back to the master. This enables the master to perform a continuity test of the

* This work was supported by the U.S. DOE contract No. DE-AC05-84-ER40150

entire link. The frequency of the message passing is AC line synchronized 60 Hz.

The message from the master to the slave timing modules contains the status and polarity of the 30 Hz perturbation signal sent to the correctors or cavities. The BPM system reads this message and performs the appropriate measurement calculations.

Since the sole usage of the fiber link is for timing synchronization and there is only one source of messages, this system guarantees synchronization to a time approximately equal to the maximum round trip time for a message. Worst-case delay from received input to re-transmitted output per module is less than 1.5usec. In a complete implementation, with up to 100 IOCs participating, the total round trip time will be 150usec. This eliminates the possibility of receiving incorrect information regarding the beam perturbation polarity.

3 TIMING MODULE

The purpose of the master timing module is two-fold. First, it produces a TTL compatible square wave at 30 Hz. Phase locked to this signal, an HP3314A function generator modulates corrector magnets or RF cavities and provides the desired beam perturbation. Second, at each transition of this square wave, the master transmits on the fiber link, a message indicating the polarity of this square wave. The slave timing module makes this information available to each BPM system. The BPM system, which gathers data at 60 Hz, tags the data with the slave supplied polarity.

The accelerator has its own 60 Hz AC line synchronized global timing reference called the Beam Sync. Numerous data acquisition systems throughout the accelerator, including the BPM system, use this signal for data acquisition. The master 30 Hz clock module also uses the Beam Sync signal in order to maintain phase synchronization with the accelerator.

In summary, the Beam Sync synchronizes, at 60 Hz, the BPM system and the master timing card. The master timing module outputs a Beam Sync phase locked 30 Hz TTL square wave to drive the function generator and provides phase information (i.e. polarity) to the BPMs, via the fiber link of this square wave.

Upon reception of a message from the master module, the slave module will issue a VME interrupt to the IOC. The interrupt request level is jumper-selectable, as is the master or slave status of the module. The interrupt vector number is software programmable and is part of the IOC's system initialization.

The clock module is a 24-bit address, 16-bit data slave with D08 vectored-interrupt capability. We have implemented the VME bus interface, twelve 8-bit

registers, and the serial message encoding/decoding in a 144-pin Altera ACEX EP1K50 Field Programmable Gate Array (FPGA) operating at 20Mhz. The device is re-programmable in place via a front-panel JTAG interface [2].

We have developed several diagnostics to ensure proper operation of this system. Software in each IOC will detect the loss of interrupts from the timing module if they fail to occur at a 60 Hz rate. This will cause the BPM software to issue an alarm invalidating 30 Hz reported data. A system expert can further diagnose the system by means of self-test software. A quick determination of fiber link status may be obtained by examining the LED on the front panel of the timing module. This LED will light if the link carrier is detected and will blink if messages are being received.

4 30 HZ MEASUREMENT SYSTEM

We have developed the 30 Hz Measurement System in order to improve machine reproducibility and reduce beam tune time. This system makes it possible to track and correct machine optics by measuring the differential response generated by perturbations of the beam.

Two types of modulation devices are used for two different types of measurement. Beam energy perturbations are induced by changing the accelerating gradient of the superconducting cavities. Transverse beam modulation is performed by adjusting horizontal or vertical air core dipole correctors. We can apply both types of modulation either at the end of the injector at an energy of 67MeV, or at the beginning of the first arc at an energy of 667 MeV, providing optics measurements of the entire machine [3]. The important feature of the system is that it is possible to induce the perturbations and make these measurements not only during the tuning of the accelerator, but also during the operations of the accelerator. This is possible because the Fast Feedback system [4] removes these small perturbations prior to beam delivery to the experiments.

The BPM system includes more than 850 BPMs, controlled by 2 different types of electronics, distributed across a network of 30 IOCs. The Switched Electrode Electronics (SEE) BPM [5] software uses the new TSS to determine the 30 Hz modulation polarity and uses this information in the data acquisition calculations. As mentioned earlier, the 60 Hz Beam synch triggers the data acquisition. The software then calculates the mean value of the beam position and the amplitude of the 30 Hz beam motion.

5 PRESENT STATUS AND FUTURE PLANS

To date, we have installed the timing modules in nine locations around the accelerator. The system has recently come on-line and at present is working as designed. Future upgrades to the module's FPGA firmware and IOC software will allow non BPM IOCs to benefit from the installation of this module. Eventually, all VME crates with IOCs (approximately 100) will have a clock module, with BPM systems having the highest installation priority.

In the very near future we will implement two additional functions within the TSS. These are absolute time of day synchronization and remote system reset capability.

We will implement time of day synchronization using a new timing module message type and using network Ethernet based TCP/IP communication. The new message type will be a time hack type message. The approach will be to broadcast, via Ethernet, to all IOCs that a time hack type timing module message is imminent and upon reception of this message, the IOCs should synchronize their time of day clocks to the time specified in this Ethernet broadcast. The IOC's on-board timer will maintain the time reference between these hacks. This system will allow time of day synchronization at sub-millisecond level.

For the future, we are investigating additional serial-data encoding methods, along with the possibility of increasing the module's on-board clock speed, which should reduce the per-board serial data latency to less than 1usec.

Since the timing module is a standard VME card, it has access to the VME bus System Reset line. Asserting this line will cause the associated IOC to reboot and all boards in that crate to reset. We plan to create a new message type that will command a timing module to assert this reset. All timing modules have a jumper-selectable eight-bit address allowing 255 unique addresses (address 0 is for broadcasting messages to which all slaves respond). Reset messages will allow targeting individual VME crates for resets. By bit mask partitioning of the addresses, it is possible to reset a subsystem of IOCS. For example, it will be possible to reset all BPM IOCs with a single command. At present, many IOCs are at inconvenient locations and must be manually reset should they crash. This feature will minimize the impact of such a crash.

REFERENCES

- [1] H. Areti, "Synchronization of 30 Hz System", http://www.jlab.org/~areti/30Hz_docs/.
- [2] T. Allison, "Versatile Data Acquisition And Controls For EPICS Using VME-Based FPGAS", ICALEPCS 2001, San Jose, CA, November 2001.
- [3] V. Lebedev, et al., "Linear Optics Correction in the CEBAF Accelerator", Particle Accelerator Conference, Vancouver, British Columbia, May, 1997
- [4] R. Dickson, V. Lebedev, "Fast Feedback System For Energy And Beam Stabilization", ICALEPCS, Trieste, Italy, October, 1999
- [5] T. Powers, "Resolution of SEE BPMs", Proceedings Of The Beam Instrumentation Workshop, Stanford, CA, May, 1998